Spring 4-22-2011

ADAPTIVE PHOTOVOLTAIC CONFIGURATIONS FOR DECREASING THE ELECTRICAL MISMATCHING LOSSES

Mohamed Amer Chaaban
University of Nebraska-Lincoln, mchaaban@unomaha.edu

ADAPTIVE PHOTOVOLTAIC CONFIGURATIONS FOR DECREASING THE ELECTRICAL MISMATCHING LOSSES

by

Mohamed Amer Chaaban

A THESIS

Presented to the Faculty of

The Graduate College at the University of Nebraska

In Partial Fulfillment of Requirements

For the Degree of Master of Science

Major: Architectural Engineering

Under the Supervision of Professor Mahmoud Alahmad

Lincoln, Nebraska

May, 2011

ADAPTIVE PHOTOVOLTAIC CONFIGURATIONS FOR DECREASING THE ELECTRICAL MISMATCHING LOSSES

Mohamed Amer Chaaban, M.S.

University of Nebraska, 2011

Advisor: Mahmoud Alahmad

Electrical mismatching losses in photovoltaic systems are of great interest to system designers. In this thesis, an adaptive photovoltaic (PV) system is proposed based on novel flexible switch matrixes that form different possible topologies. This system maximizes the generated power in real-time for utility interactive systems in a modified inverter configuration. The proposed system uses fewer components and achieves maximum efficiency during shading and module mismatches by reconfiguring the PV modules based on real-time solar insolation, current operational conditions, and maximum efficiency criterion. Simulation tools are used to demonstrate that the proposed topologies provide improvement in efficiency over existing traditional PV systems. Furthermore, a prototype has been designed and developed. Experimental results for efficiency comparison between traditional PV system configurations are described in this work. Potential improvement using the proposed adaptive configuration is analyzed. The overall results validate the adaptive system and its benefits for a wide range of applications.

Acknowledgements

Thanks for the one who is the reason of me being able to achieve this work.

I would like to thank my advisor, Professor Mahmoud Alahmad for his continuous helpful and inspiring feedback throughout the period of my MS studies.

I would also like to thank the committee members Professor Clarence Waters and Professor Dale Tiller; and the Environmental Protection Agency [EPA] for funding this project.

My appreciation is also extended to all colleagues in Architectural Engineering for their help and their support.

The last but not the least, I would like to show my deepest gratitude and respect to my family, especially my parents, the ones to whom I owe all success in my life.

Table of Contents

List of Figures

List of Tables

1. Introduction

1.1. General

This chapter presents the motivation of the research tackled in this thesis. The chapter also provides the main objectives of the research and outlines each chapter.

1.2. Motivation

Currently, two major and global interrelated energy problems face the world. The first problem is that the world economy is based on fossil fuels, mainly oil. However, the world's oil fields are depleting. At the same time demand for oil is expected to grow rapidly. These issues could lead to a major economic crisis. The second major problem is climate change (1). Due to the environmental issues caused by the over-reliance on fossil fuels as prime energy source of everyday activities and while the world population and energy consumption increase, electricity production is a leading cause of air, land, and water pollution. Recent studies predict that the world's net electricity generation increases from 18.8 trillion kilowatt-hours in 2007 to 25.0 trillion kilowatt-hours in 2020 and 35.2 trillion kilowatt-hours in 2035 (2). In order to overcome the problems associated with generation of electricity from fossil fuels, the interest in renewable energy stems from the desire to play a part in helping build a "greener" and more energy sustainable future for our planet. Renewable energy resources are abundant, clean, cost efficient, and do not emit harmful CO_2 gases. Solar energy, wind energy, hydro energy, geothermal energy, tidal energy, and biomass are clean sources of renewable energy. The sun is an infinite energy reservoir. In other words, solar energy is the most abundant energy resource on earth. "The solar energy that hits the earth's surface in one hour is about the

same as the amount consumed by all human activities in a year (3). The sun light can be converted to electricity using the photovoltaic effect. The use of photovoltaic (PV) systems for electricity generation started growing rapidly worldwide.

There is currently a growing trend towards the more widespread use of solar energy systems. As of yet, few photovoltaic-systems have been implemented into grids due to their relatively high cost and modest efficiency. Although the efficiency of PV panels is currently still poor and its use is small. Solar photovoltaic (PV) power has a particularly promising future. The global PV market has experienced vibrant growth for more than a decade (since 2000) with an average annual growth rate of 40% and it has significant potential for long-term growth over the next decades. The cumulative installed PV power capacity has grown from 0.1 GW in 1992 to 14 GW in 2008. Annual worldwide installed new capacity increased to almost 6 GW in 2008 (3). Figure 1 illustrates the global cumulative installed capacity of PV for the past two decades. Today, PV provides 0.1% of total global electricity generation. However, PV is expanding very rapidly due to dramatic cost reductions. In the IEA solar PV roadmap 2010 vision, " PV is projected to provide 5% of global electricity consumption in 2030, rising to 11% in 2050.This roadmap envisions that by 2050, PV will provide 11% of global electricity production (4500 TWh per year), corresponding to 3000 giga-watts of cumulative installed PV capacity". This will help to avoid 2.3 giga-tonnes (Gt) of CO2 emissions per year (3). IEA targets to reach a 50% CO2 emission reduction by 2050. a recent survey presented also by the International Energy Agency (IEA) reports that over 2.26 GW of PV capacity was installed during the year 2007 in the IEA participating countries. For example, Germany has (5.3 GW) installed capacity, Spain (3.4 GW), Japan (2.1 GW) and the US

(1.2 GW). Almost 80% of the total global capacity is provided by these countries. Other countries are getting involved into the PV market through implementing new policies and incentives (3).

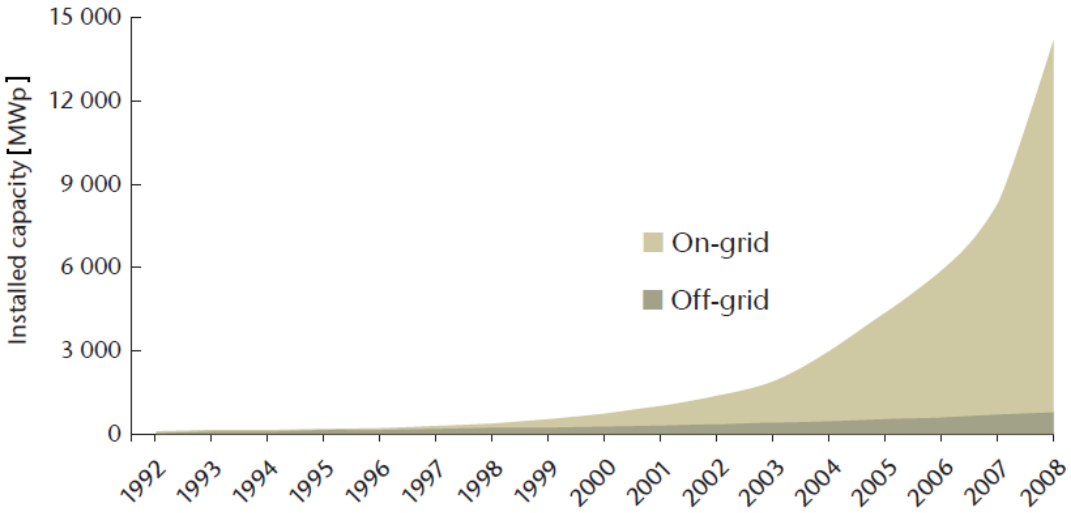

Figure 1: Cumulative installed global PV capacity (3)

1.3. Problem formulation

PV systems are usually used in two main fields: 1) off-grid applications, stand alone system, operate autonomously and supply loads without any connection to the utility, and; 2) grid-tied, or grid connected applications, in which solar arrays are used to supply energy in parallel with the utility to local loads as well as to the electric grid.

These two types are implemented according to IEA solar PV roadmap into four end-use sectors with distinct markets for PV as following:

Residential systems (typically up to 20 kW systems on individual homes); Commercial systems (typically up to 1 MW systems for commercial office buildings, schools,

hospitals, and retail); Utility scale systems (starting at 1 MW, mounted on buildings or directly on the ground); Off-grid applications (varying sizes).

All sectors are growing rapidly and PV technology will play a significant role in the future electrification. For example according to IEA roadmap, 11% of the global electricity generation is to be provided from PV system by 2050.

One of the major issues that faces the widespread use of PV systems is the installation of large systems (megawatt systems) that might lead to some technical problems in the electrical coupling with the utility such as safety – unintentional islanding, and Power quality – voltage rise (1).

Another major obstacle that faces PV installation is the high initial cost, which is reflected in the cost per KWh of the energy produced by PV systems. This obstacle can be overcome by developing low cost PV (3) cells and by providing incentives to customers that tend to install these systems.

Another problem that faces PV system especially in commercial and residential sectors, which is the main focus of the research presented in this thesis, is the electrical mismatching losses between the system components, such as PV modules and power conditioning units, during abnormal operational conditions (i.e. shading and low radiation conditions). These losses occur as a result of unequal voltage and current of the PV modules. A solution for solving this problem is by accurate design of the configuration that gives better matching between the PV system's components.

Another approach to solving this associated problem is developing a smart design and configuration that can overcome these mismatching losses using a number of additional

components such as switches. This leads to the concept of the adaptive system that changes the configuration according to current the operational condition. This helps finding the optimal possible configuration, thus, minimizing the mismatching losses.

1.4. Research Objective and Methodology

The goal of the research presented in this thesis is to decrease the electrical mismatching losses in the PV system. This goal can be achieved by evaluating the performance of the traditional PV system configurations and by investigating the mismatching losses of different methods that is used to improve the performance of the PV system, especially during different operational conditions.

The main objectives of the research can be summarized as follows:

1. Develop a method that determines the losses in the PV output power. The method used in such a study can provide accurate evaluation of the possible impacts by covering the following aspects:

- Estimate the profile of the output power of the PV system (P-V curve) using simulation tools for different irradiance and shading conditions and for different PV configurations.
- Perform practical experiments that give an actual performance analysis of the traditional and the proposed PV system configurations.
- Apply statistical analysis in order to identify the mismatching losses. Hence, proper operational configurations can be proposed to solve the expected problems.

2. Develop solutions to reduce the mismatching losses impacts. The steps include:

- Propose a flexible switching matrix [FSM] that can be implemented in the system to allow multiple configuration formations.
- Evaluate the current performance of string-inverter and micro-inverter configurations and proposing an adaptive PV-inverter configuration using [FSM].
- Select the suitable location for installing the system, from a number of candidate locations.
- Evaluate the current performance of central-inverter and multi-DC/DC configurations and proposing an adaptive PV configuration using [FSM] and an additional DC/DC converter using MATLAB model and practical experiments.
- Propose a revised version of adaptive PV strings configuration using an economical number of switches in the [FSM], thus improving the potential of using adaptive PV system.
- Study the potential of developing the adaptive PV system and [FSM] with adaptive energy storage devices, such as batteries, to control the energy captured for PV during different operational conditions.

1.5. Work Structure (thesis outlines)

This thesis is structured as following:

Chapter 2 provides a general overview of photovoltaic (PV) concept including the radiation received from the sun, the PV effect (the electrical conversion technology), PV cell basic characteristics, PV system types, and PV applications.

Chapter 3 discusses the components of a grid-connected PV system and the current connection topologies. The chapter also discusses the critical issues that faces PV system in the practical installations.

Based on the review of current PV topologies in chapter 3, chapter 4 introduces the layouts of the new adaptive photovoltaic topologies. This chapter also discusses the Flexible Switching Matrix in details and discusses different proposed PV topologies such as Adaptive PV central-inverter configuration, Adaptive PV-inverter topology, and the Adaptive PV string-inverter configuration including some illustrations of different operational conditions and the controller logic.

In chapter 5, analyses of the performance of the traditional and adaptive configurations are presented. Simulation and practical models are used as verification methods. Furthermore, results of both systems are analyzes and compared.

Finally, in chapter 6, the summary and conclusion s of the thesis are presented. Moreover, a potential research idea for future work in this field is proposed.

2. Photovoltaic, an overview

2.1. Introduction

It is difficult to understand the photovoltaic effect without basic knowledge of the solar energy source. For the purpose of this research, the radiation received from the sun, and the effects of the atmosphere on the radiation are introduced. Then, the photovoltaic effect (the electrical conversion technology), PV cell basic characteristics, PV system types, and PV applications are discussed in this chapter.

2.2. Solar Energy

Solar energy is considered to be one of the three main energy resources that are solar energy, geothermal energy, and tidal energy. The sun is a vast and hot sphere of gas. It has an effective black-body temperature of 5777 K (Kelvin) and it is the largest member of the solar system. The Sun is a sphere of intensely hot, gaseous matter with a diameter of 1.39×10^9 m and is, on average, 1.5×10^{11} m away from the Earth (4). The energy of the sun emerges from fusion reactions where four hydrogen nuclei fuse into one helium nucleus in the hot interior of the sun. The maximum spectral intensity occurs at about 0.48 μm wavelength in the green portion of the visible spectrum as shown in Figure 2. About 8.73% of the total energy is contained in the ultraviolet region (0.40 μm); another 38.15% in the visible region (0.40 μm to 0.70 μm) and the remaining 53.12% in the infrared region (0.70 μm).

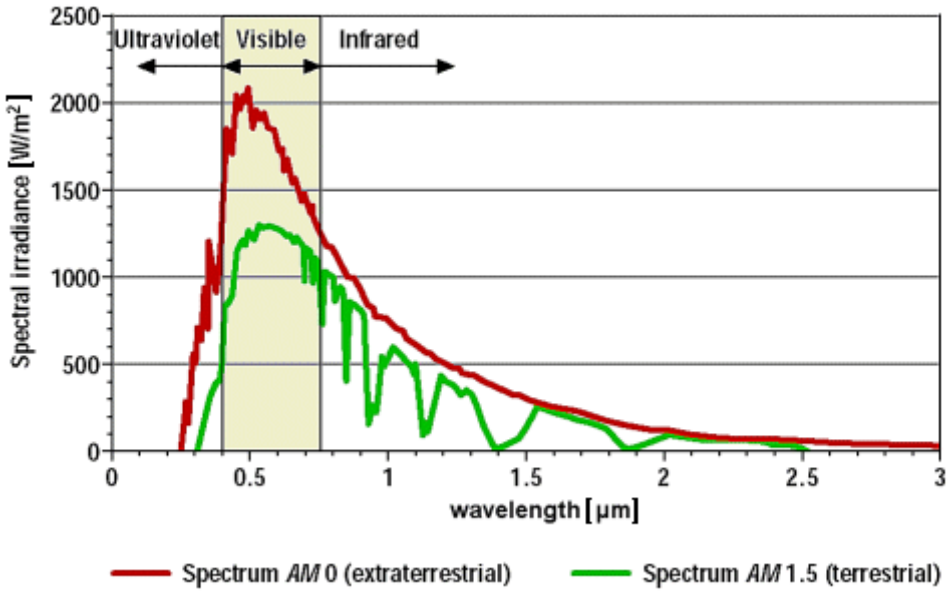

Figure 2: Extraterrestrial and Terrestrial Spectrum of Sunlight (5)

2.2.1. Solar Radiation on the Earth's Surface

The Earth orbits around the Sun once every 365.25 days. Nearly two-thirds of the Earth is covered by water and the remaining one-third is land. Half of the Earth is lit by sunlight at a time. As the solar radiation reaches the atmosphere of the earth, the Earth's atmosphere absorbs the ultraviolet (UV) and infrared radiation and allows only radiation having wavelength ranging between 0.29 µm and 2.3 µm, known as short wavelength radiation (4).

The extraterrestrial radiation is the radiation that passes perpendicularly through an imaginary surface just outside the earth's atmosphere. Depending on the distance between the sun and the earth, the radiation varies. The amount of solar radiation that is absorbed or scattered in the atmosphere depends on the path length of the sun's rays through the atmosphere; this quantity is called the air mass (AM) ratio. It is the ratio

between the length of the actual path taken by the rays and the minimum path length, i.e., the path length when the sun is at the zenith. Zenith is the point in the sky directly overhead the location, by definition, AM =1 when Zenith = 0 at sea level while AM=0 outside the atmosphere (6). AM=1.5 is considered to represent the average terrestrial radiations in US. Figure 3 illustrate the AM according to Zenith.

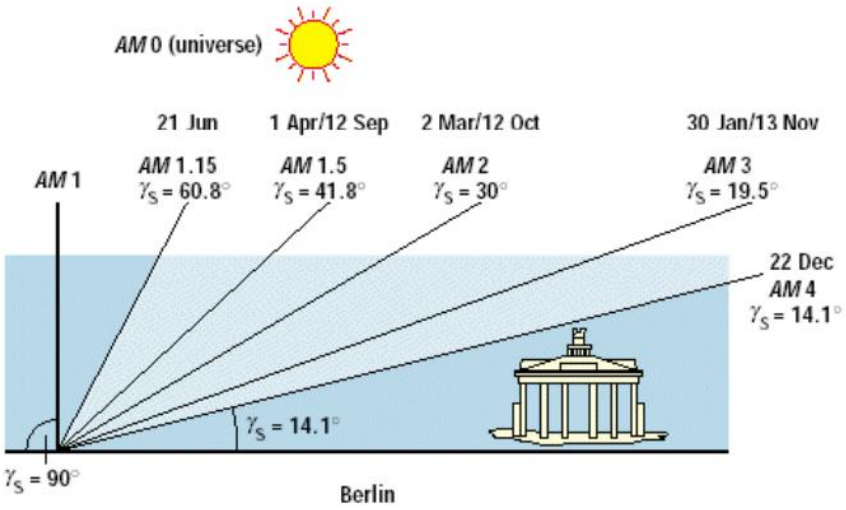

Figure 3: Position of the Sun and AM values at solar noon for various days in Berlin, Germany (5)

Irradiance or insolation is the instantaneous solar power received on a unit surface area and is normally given in Watt per Meter square (W/m^2). The *global irradiance*, G_g, the solar radiation that reaches horizontal surface on the earth through the atmosphere, the terrestrial radiation, is classified into two components: beam and diffuse radiation.

Beam radiation (I_b): is the radiation that passes in a straight line through the atmosphere to the surface. It is also known as Direct radiation.

Diffuse radiation (I_d): is the solar radiation scattered by aerosols, dust, clouds and molecules. Another source of the diffused radiations is direct radiation that reaches the

ground and is reflected back up through the atmosphere. Diffuse radiation can reach the surface from any direction.

Total radiation (I_t): is the sum of the beam and diffuse radiation, sometimes known as *global radiation*. For more information about the solar radiation and solar angles see Appendix A.

2.3. Photovoltaic Technology

Solar energy can be used in different ways. Direct conversion of sunlight into electricity in PV cells is one of the three main solar active technologies, the two others being concentrating solar power (CSP) and solar thermal collectors for heating and cooling (SHC). The following subsections describe the photovoltaic definition, photovoltaic effect, the basic parameters of the solar PV cell, modeling of PV cell, the concept of module/panel/array, PV system types, and finally the applications of PV systems.

2.3.1. The Photovoltaic

PVs use special semiconductor materials to utilize the solar energy by converting it to an electrical energy. Doping two different semiconductor materials by different imputes forms two types of semiconductor layers that are used to fabricate solar cells. This connection is called (p-n junction), which is the basic building block of the PV system. This semiconductor is the material that can conduct electricity when the temperature raises or when exposed to light. Solar cell or PVs cell directly convert the solar energy into electricity by the photovoltaic effect. This phenomenon is similar to the photosynthesis in the plant that converts the sunlight into bio-energy. The commercial

solar cell is made of wafer-based technology of semiconductor materials, such as Crystalline Si (C-Si) and thin film. Different types of silicon can be used to fabricate the solar cell *i.e.* mono-crystalline silicon, poly-crystalline silicon, and amorphous. The variation between these types is distinguished by the conversion efficiency of the PV cell. There are other technologies becoming known such as concentrating PV (CPV) and organic cells. These two technologies have the potential to reduce costs and improve efficiency. Generally, solar cells generate small amounts of power because of the limitations of the surface characteristics. (For more information about PV material technology, refer to Appendix B).

2.3.2. Photovoltaic Effect

When irradiance hits the surface of solar PV cell, an electrical field is generated inside the cell. As can be seen in Figure 4, this process separates positive and negative charge carriers in an absorbing material (joining p-type and n-type). In the presence of an electric field, these charges can produce a current that can be used in an external circuit. This generated current depends on the intensity of the incident radiation. The higher the level of light intensity, the more electrons can be unleashed from the surface, the more current is generated.

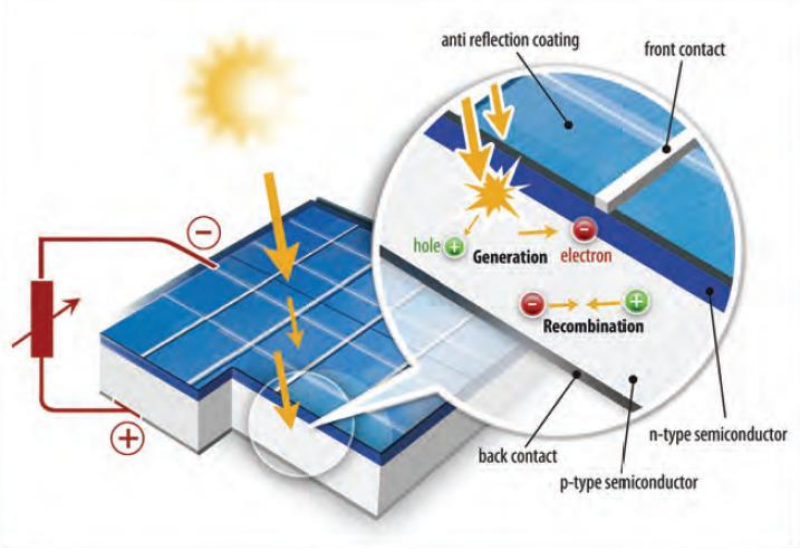

Figure 4: Schematic cross-section of a typical solar cell (1)

2.3.3. Basic Parameters of Solar PV Cell

Normally, the electrical characteristics of a PV cell are displayed as a relation between the cell voltage and current, and a relation between the cell voltage and power. However, several electric quantities are important to describe the operation of the PV cell. These electric quantities include: the cell voltage under open circuit conditions, V_{OC}, the cell current under short circuit conditions, I_{SC}, and the cell voltage, current and power at the maximum power point, V_{MPP}, I_{MPP}, and, P_{MPP}, respectively.

2.3.3.1. Current-Voltage (I-V) Characteristics

I-V characteristics curve represents all possible current and voltage operating points for PV cell. This curve can be generated by changing the electrical load value during lab experiment. As can be seen in Figure 5, when voltage increases, the current start at its maximum value then decreases gradually to reach the zero. The operating point at I-V curve is determined by the electrical load.

Certain points at the I-V curve are highlighted to rate the PV module performance and are used for the design of PV systems. These measured values are taken at the Standard Test Condition (STC), which are at irradiance (G= 1000 w/m^2), Temperature (T= 25 ^{o}C), and Air Mass (AM=1.5). The knee points, in both I-V and P-V, represent the maximum power point, which is at 0.5 V and 2.75A in Figure 5. The optimum electrical load is the load that operates the PV at its maximum power point (MPP), if the PV generator is able to deliver maximum power.

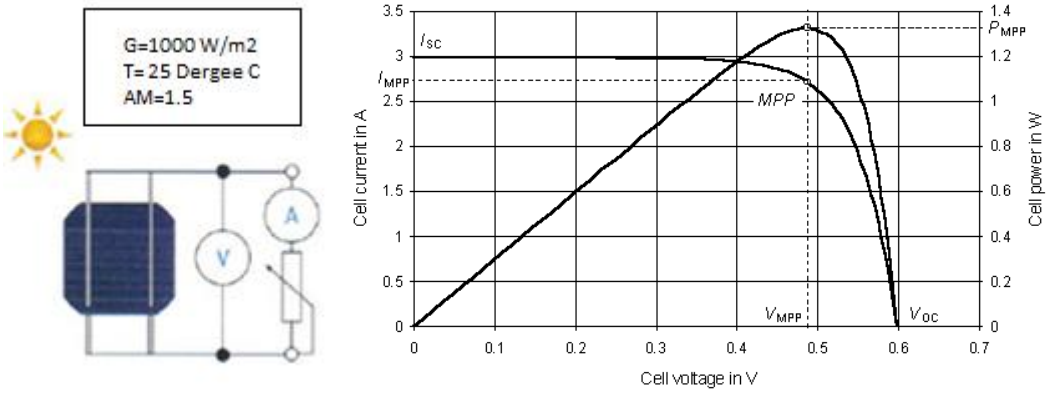

Figure 5: Current–voltage and power–voltage solar cell characteristics (5, 7)

The electrical characteristics of the PV cell depend on the irradiance and the cell temperature. As in Figure 6, there is a proportional relationship between the current and the irradiance at different levels of the irradiance and constant temperature. Figure 6 (a) and (b) show that any change in irradiance has a strong effect on the short-circuit current and the output power of the solar cell, but negligible effect on the open-circuit voltage. On the other hand, Figure 6 (c) and (d) shows that any change in the temperature at constant irradiance has a significant effect on the open-circuit voltage and output power of the cell, while negligible effect on the short-circuit current.

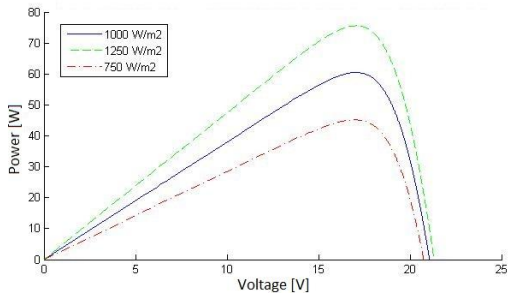

(a) Variable Irradiances and constant Temperature

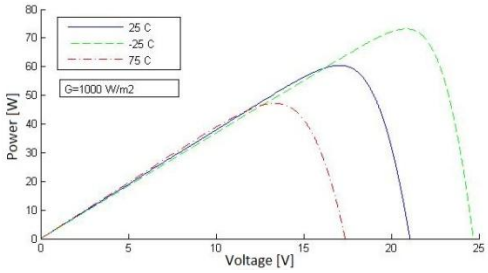

(c) Variable Temperature and constant Irradiances

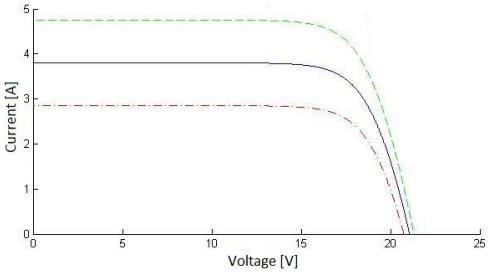

(b) Variable Irradiances and constant Temperature

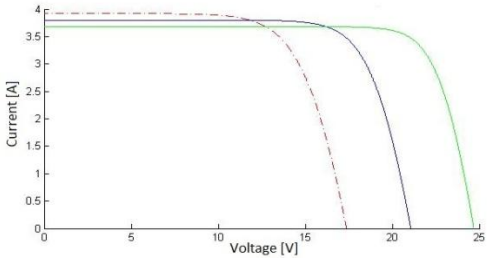

(d) Variable Temperature and constant Irradiances

Figure 6: the temperature and irradiance effect on the open-circuit voltage and output power of the cell generated by MATLAB

2.3.3.2. Short Circuit Current (I_{SC})

Short circuit current is the maximum possible current in the circuit, at zero voltage as shown in Figure 5. In other words, when there is negligible electrical load in the circuit. This case occurs by connecting the positive and negative terminals together. The short circuit current is directly proportional to the available sunlight (8).

2.3.3.3. Open Circuit Voltage (V_{OC})

Open circuit voltage is the maximum voltage, at zero current (8). In other words, open circuit voltage represents the maximum possible voltage value, which occurs when a huge load in connected to the circuit or in case of no load (4).

2.3.3.4. Maximum Power Point (P_{MPP})

In case of short circuit or open circuit operating points, no power is generated. As a result, the operating point should fall into the range of the maximum power output of PV cell as shown in Figure 5. This operating point is determined by choosing the correct value of the connected load. The maximum power output is defined as the multiplication of the voltage and the current at the MPP:

$$P_{MPP} = V_{MPP} \times I_{MPP} \qquad (1)$$

Where V_{MPP} and I_{MPP} are voltage and current the values that gives the maximum operating power.

MPP is the rate of the unit by W_p (watt peak) (8) (4).

2.3.3.5. Fill Factor (FF)

The fill factor is an indicator of the quality of the PV cell. The sharpness of the knee in an I-V curve (e.g. Figure 5) indicates how well a (p-n) junction is manufactured (7). The maximum value of the fill factor is one, which is theoretical value only. The maximum practical value in silicon is 0.88 (4). FF is defined as the ratio between the maximum generated power at MPP and the maximum theoretical power (I_{sc} multiply by V_{oc}).

$$FF = \frac{P_{max.practical}}{P_{max.theoretical}} = \frac{V_{mp} \times I_{mp}}{V_{oc} \times I_{sc}} \qquad (2)$$

For a good I-V curve profile with fill factor close to unity, the current should stay constant while the voltage increases till the operating point reach the knee of the curve. After that point, the current of PV cell should also gradually decrease.

2.3.3.6. Efficiency of Solar Cell

Only part of the solar radiation incident on the solar cell is converted to electricity. The conversion efficiency of PV cell is defined as "the ratio between the produced electrical power and the amount of incident solar energy per second" (3).

The equation of solar cell power conversion efficiency is:

$$\eta = \frac{P_{max}}{P_{in}} = \frac{I_{max} \times V_{max}}{Incident\ solar\ radiation \times Area\ of\ solar\ cell} = \frac{V_{oc} \times I_{sc} \times FF}{I_t \times A_c} \quad (3)$$

Where I_{max} and V_{max} are the current and voltage for maximum power, corresponding to solar intensity I_t (4). **Error! Reference source not found.** illustrates the relationship between the FF and the efficiency of the cell.

2.3.3.7. Threshold Voltage (V)

Unlighted PV cells form diode characteristic.

Figure 7 shows the (I-V) characteristics of the diode. As can be seen, the diode has threshold voltage to allow the current to flow through it (the 1st quadrant of the (I-V) curve of the diode). This process is also known as *forward bias*. There is another kind of bias of the diode (the 3rd quadrant of the (I-V) curve of the diode) which is called *reverse bias*. This last allows very small current to flow through the diode when the voltage is applied in the reverse direction of the diode. In case of illuminated PV cell, the (I-V) characteristic curve of the diode is shifted, by the magnitude of the generated current from the p-n junction, in the reversed current direction (the 4th quadrant of the (I-V) curve of the diode) (4, 7).

Figure 7 illustrates the characteristics for both of lighted and unlighted PV cell.

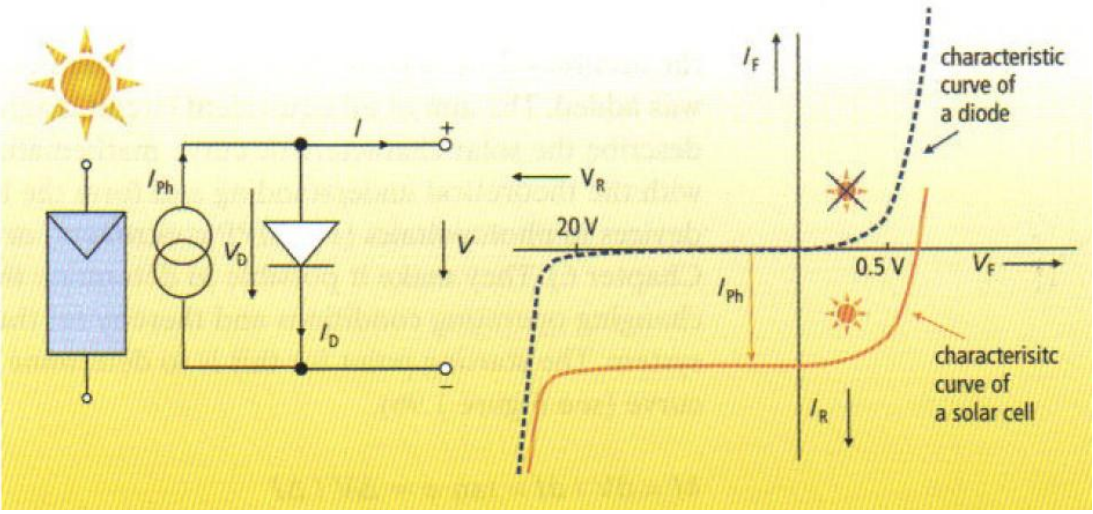

Figure 7: the electrical characteristics of lighted and unlighted PV cell (7)

2.3.3.8. The Equivalent Circuit of PV Cell

When the p-n junctions are formed, a diode is also formed as a result of this junction. In other words, PV cell is current source including a diode formed by joining different types of semiconductors (p-type and n-type). The electrical analysis of the PV cell includes a source which is the sun and unique equivalent electrical circuit which includes diode and series and parallel resistances (4).

Most studies related to the performance of PV systems require a model to represent the performance of the irradiance received by the PV array and ambient temperature that are being converted into DC power output of the PV array, (P_{MPP}). The models recorded in the literature vary in accuracy and complexity. The single-diode model shown in Figure 8 is one of the most popular physical models used to represent the equivalent electric circuit of a single PV cell (7)(4).

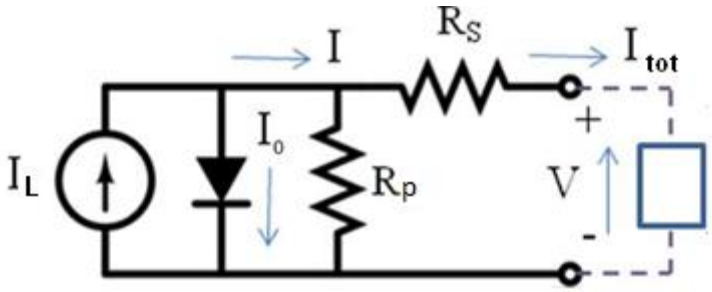

Figure 8: the equivalent electric circuit of a single PV cell

The ideal cell model consists of: 1) the ideal current *I* which is equal to the current I_L generated by the photovoltaic effect minus the diode current I_D, according to the equation:

$$I = I_L - I_D \qquad (4)$$

While:

$$I_D = I_0 \left[exp(eV/kT) - 1\right] \qquad (5)$$

Where I_0 is the saturation current of the diode, e is the elementary charge 1.6×10^{-19} Coulombs, k is a constant of value 1.38×10^{-23}J/K, T is the cell temperature in Kelvin, and *V* is the measured cell voltage (4). 2) a shunt diode representing the p-n junction of the PV cell, 3) a shunt resistance, R_p, accounting for the leakage currents due to the impurities of the p-n junction (the value of this resistance should be made as high as possible), and 4) a series resistance, *Rs*, representing all the distributed Ohmic resistances in the semiconductor and the resistances of the metallic contacts (ideally, the value of this resistance should be zero). **Figure 9** shows the effect of changing the value of these resistances on the I-V curve of a PV cell. The following equation describes the equivalent mathematical model of the PV cell:

$$I_{tot} = I_L - I_0 \left[exp\left(\frac{e(V - IRs)}{AkT}\right) - 1\right] - \left(\frac{V - IRs}{Rp}\right) \qquad (6)$$

Where: I_{tot} is the total current of the real PV cell including all losses in the diode and the shunt resistor $R_{p;}$ and A is constant usually =1.

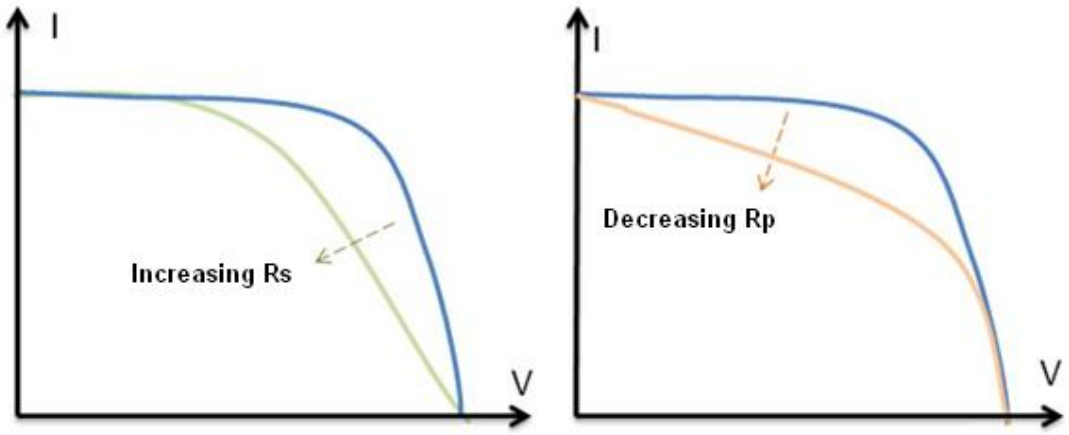

Figure 9: Series and parallel resistances in PV cell (9)

2.3.4. Modeling & PV System Simulation

Manufacturers of PV modules provide the most important information about module characteristics such as maximum power point voltage, and current and power output at standard test conditions (STC). This information is used to simulate the Current-Voltage (I-V) and Power-Voltage (P-V) curves. The current in the equivalent circuit of the PV cell can be expressed as a function of the module output voltage. In (10) and (11), a new approach to simulate I-V and P-V curves was achieved for the single scale level. This scale may be a PV cell, module, or array. Using the important characteristics of the PV cell that are open circuit voltage, short circuit current, and the maximum power point

voltage and current, the model can generate satisfactory results. While this model is used to simulate simple cases of PV system, it is not sufficient to simulate a real PV system with different operational condition such as shadowing effect across some modules in the string or parallel strings with different operation conditions. In this case, the model will not be able to simulate all required cases of the adaptive system.

To solve this problem, another simulation model, (the model used in this work), is developed in (12). Implementing this model, the simulation of the whole PV array can be achieved. The model is based on a group concept. This allows simulating the real array cases of different isolation and shadowing effects. The inputs of each group are adjustable. Solar irradiance, temperature, and the number of parallel strings in each group are considered as inputs. Shaded modules are also considered in this case. A special group will take care of simulating this effect in the PV array. This simulation tool will be used in the following chapter that study the behavior of the traditional PV systems and it will also be used to simulate the performance of the proposed PV system configurations.

2.3.5. Module/ Panel/ Array

In order to implement the cell into real application, a combination of cells forms different sizes where a module consists of connected PV cells in one frame, and an array is a complete PV unit consisting of connected modules with structural support (6). Each PV array is comprised of parallel connected strings. Each string consists of multiple series connection of PV modules that provide the required voltage of the array. These structures can be used to supply power to scalable applications known as photovoltaic plants, which may be stand-alone systems or grid-connected systems (4).

2.3.5.1. Series Parallel Connections of PV Modules.

PV cells are first connected in series in most manufacturing methods to form PV module. Modules can be connected in different ways to form PV array. This is done for the sake of voltage/current requirement of the power conditioning units (PCU's) of the PV system. In order to do that, a series and parallel connections of PV modules are needed.

2.3.5.1.1. Parallel Connection

Figure 10 shows the parallel connection of PV modules to create a PV array. As can be seen, the negative and positive terminals of the first module are connected to negative and positive terminals of the second module. If higher currents are demanded in a system, parallel connection of the individual strings can be used, as is shown in Figure 10. In a parallel connected configuration, the total current is equal to the sum of the individual current of each PV modules. In this case, the output voltage is equal to the voltage of the single PV module (4, 7).

$$V_{out} = V_1 = V_2 \dots \dots = V_n \qquad and \qquad I_{out} = \sum_{i=1}^{n} I_i \quad (7)$$

As a result, the output power of the solar array is given by:

$$P_{out} = I_{out} \times V_{out} = V_{out} \times \sum_{i=1}^{n} I_i \qquad (8)$$

Where: I_i is the current of the string i,

It is the most robust configuration for a solar array under low radiation and shadow conditions.

Any similarity between the current values of the parallel connected modules should be taken into account to avoid the electrical mismatching losses of the system (6, 8).

2.3.5.1.2. Series Connection

To create a higher DC output voltage, solar modules are often connected in series. As can be seen shown in Figure 10 the negative terminal of the first module is connected to the positive terminal of the second module and so on. This forms a string with two main terminals, which are the positive of the first modules and the negative of the last one. Here, the same current flows through every solar cell, and the total voltage is the sum of the partial voltages across the individual modules (4, 7). The output voltage and output power of the string of the series-connected solar cells are:

$$I_{out} = I_1 = I_2 \dots \dots = I_n \qquad and \qquad V_{out} = \sum_{i=1}^{n} V_i \qquad (9)$$

As a result, the output power of the each string is given by:

$$P_{out} = I_{out} \times V_{out} = I_{out} \times \sum_{i=1}^{n} V_i \qquad (10)$$

Where: V_i is the voltage of the module i,

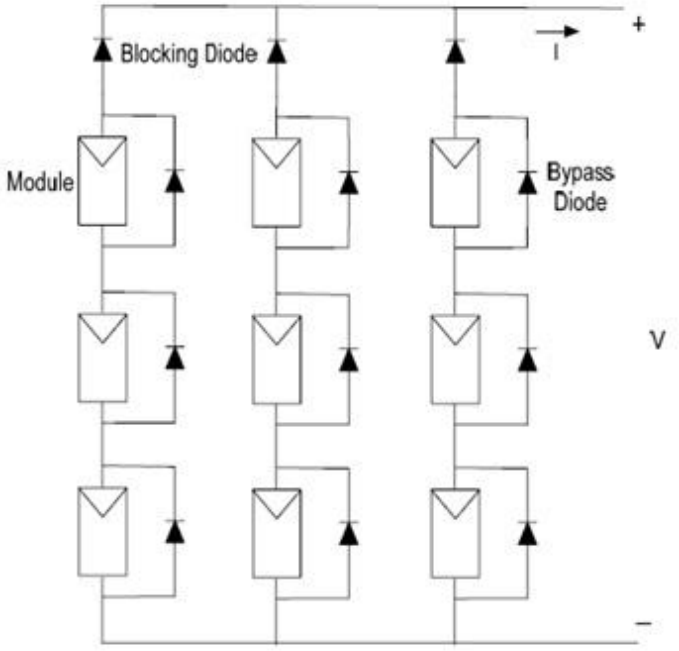

Figure 10: PV array consisting of series and parallel PV modules

Similarity between the voltages of the series connected modules should be taken into account to minimize the electrical losses of the system (6, 8).

Series connection of the solar cells and also of the solar modules causes an undesired effect when a solar cell or module is fully or partly shaded. The weakest link in the chain determines the current of the whole string. Even when only one cell is (partly) shaded, the effect is the same as if all the series connected cells or modules were shaded. In this way the power output drops drastically. And a shaded module or cell will act like a load, thus increasing the temperature in it and sometimes create so-called "hot spots" that damage the shaded cell. To avoid this operating condition, bypass diodes are connected anti-parallel to the solar modules as shown in Figure 10. The ideal solution is with one such bypass diode for each solar cell. However, in practice, it is sufficient to provide one bypass diode for every 15 to 20 solar cells (4).

2.3.6. PV System Types

2.3.6.1. Introduction

Due to the fluctuation of the solar radiation, energy generated from PV systems doesn't always meet the temporary energy demand of the end users. Thus requiring additional energy solution such as energy storage system (batteries) or sometimes requiring alternative energy sources such as hybrid systems. Many different types of PV systems have been practiced. The choice of the optimal system type for particular location depends upon geographical, economical and technical factors. In general, the PV system configurations fall into four main types: Stand-alone systems (off-grid); utility interactive systems (grid- connected); bimodal system (battery-based interactive system); and the hybrid system. The last configuration can be categorized into the first two types.

2.3.6.2. Stand Alone System

Stand alone systems operate autonomously to supply loads without any interaction with the utility. This system can be configured in a variety of ways as shown in Figure 11. It can be configured as a direct coupled system in which the PV is directly connected to the load, as a self regulated system in which energy storage (the battery) is added but with no active control to protect it except through careful system design, or as a charge controlled system in which a charge controller is added for battery management.

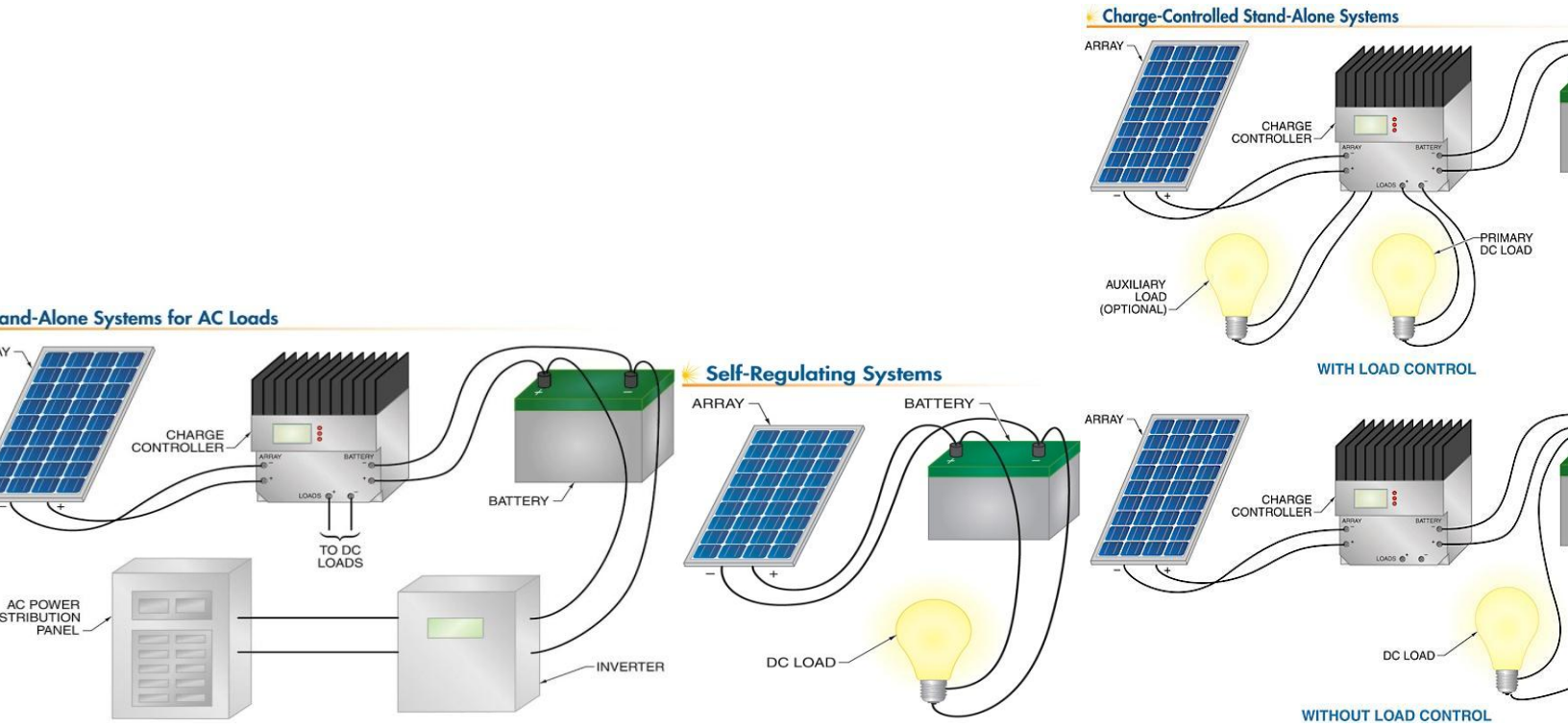

Figure 11: Stand Alone System Types (6)

Stand alone systems can operate in parallel with other energy sources, in this case the system is called hybrid systems, which is also discussed later in this section. These systems are used in isolated areas that are not connected to utility supply (7) (6).

2.3.6.3. Utility Interactive System

Utility Interactive Systems (UIS) are used in parallel with the public utility that is considered to be the infinite storage of the generated energy. UIS consists of PV array and power conditioning units (PCUs) that supply the power to the utility as shown in Figure 12.

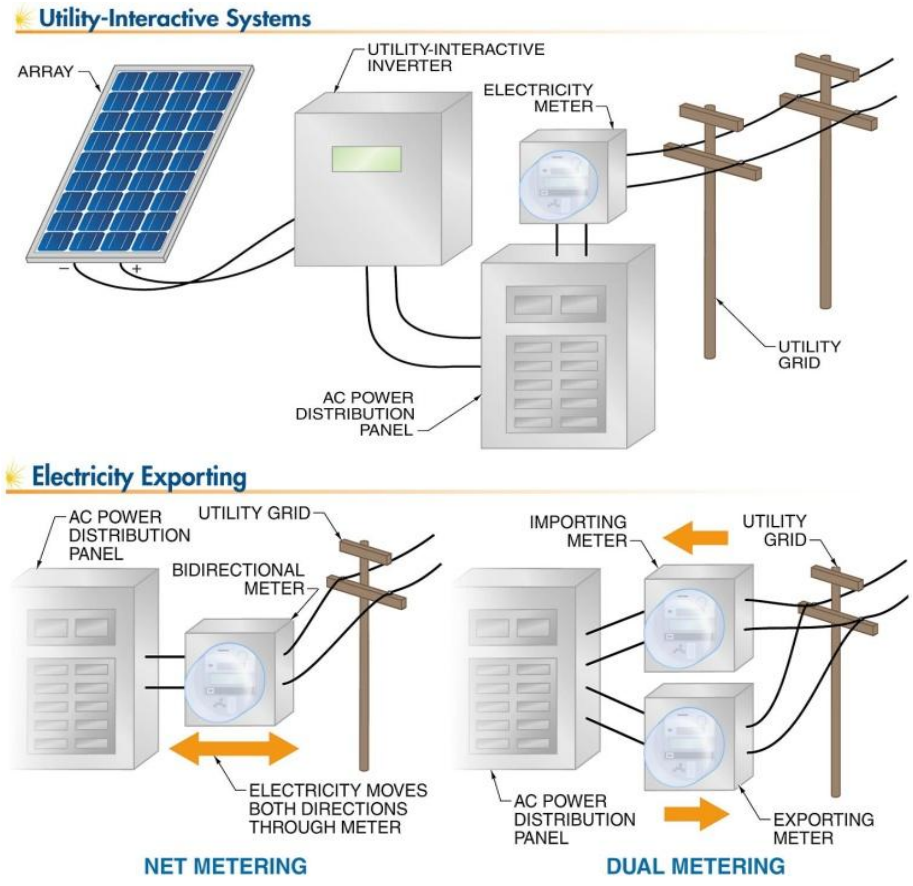

Figure 12: Utility Interactive System and Metering Types (6)

As discussed in Chapter 1 (Figure 1), most of the residential applications are going to be grid-tied systems in the next decades. In this case, the customers can import extra energy from the utility in case the PV system does not generate enough energy or feed the

excessive PV energy to the utility especially in the day time where more sun radiation is available. As a result, a metering system should be used to measure the actual energy consumption. One option is to use *Net metering* that runs backwards when the energy is exported from the utility to the end user. Another method is the dual metering that uses two separate metering devices to detect the energy consumed and generated. This method is used especially in large PV installations. Both methods are shown in Figure 12. They require the utility to have special sale prices or credit system (7) (6).

2.3.6.4. Bimodal System

Bimodal PV systems operate as stand-alone or as utility interactive systems. These use battery banks to supply the load or the utility. Storage devices are used to improve the availability of the power generated by the PV system. As can be seen in Figure 13, the key component of this system is the inverter. It always keeps the battery fully charged. In normal operational conditions, the PV array charges the battery and supplies the excessive power to the load or the utility grid. In case of utility outages, the inverter disconnects the utility connection point and the system acts as a stand-alone system where batteries supply the load. In case of no solar radiation and the battery needs charging, the inverter will draw energy from the utility to keep the battery fully charged (7) (6).

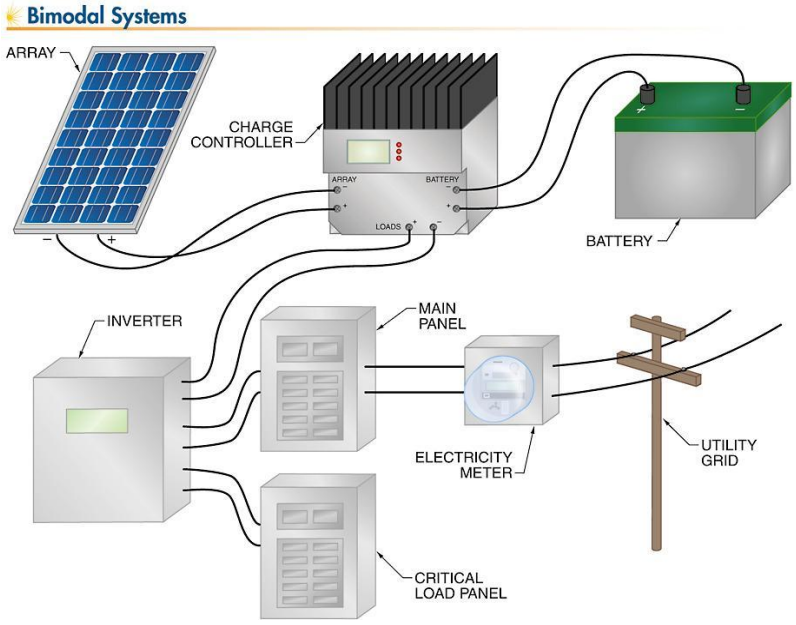

Figure 13: Bimodal System (6)

2.3.6.5. Hybrid System

Hybrid systems are systems that incorporate multiple distributed energy sources such as the PV, wind turbine, battery banks, hydro-power, and engine generators, depending on the availability and cost of different energy sources (6), (13), (7). Figure 14 illustrates the components of the hybrid system.

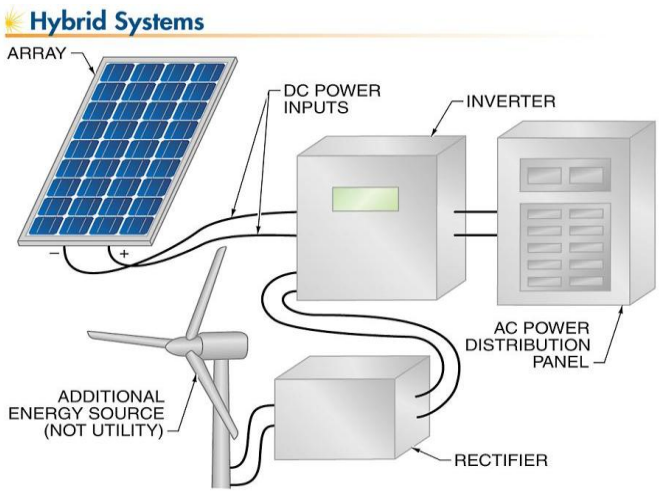

Figure 14: Hybrid System (6)

2.3.7. PV Applications

Starting with space applications, one of the most important energy source in the space shuttles is the solar energy. In the building sector, Building Integrated Photovoltaic (BIPVs) are mounted on the roof or walls of buildings. These are increasingly incorporated into new building design and are one of the fastest growing segments of the photovoltaic industry. PVs are also being used increasingly to provide auxiliary power in boats and solar cars. Recent technologies can also help produce hydrogen, making them one of the top prospects for alternative energy for automobiles. For a small application, PV has been used to power calculators and portable devices. There are also used in parking meters, emergency telephones and temporary traffic signs. While water demand increases during dry days when plenty of sunshine is available, water pumping is a considered to be a very suitable application for solar PV. For outdoor applications, solar PV street lights can be used as yard lighting, street lights, or compound lights. The photovoltaic modules charge the batteries during the day time and then use it for night illumination (7) (4).

3. Grid-Connected PV Systems

3.1. Introduction

Most of PV installations tend to be grid-connected systems as discussed in chapter 1. System components and different connection topologies are discussed in this chapter.

3.2. Components of Grid-Connected PV Systems

Grid-connected PV systems generally consist of three main components; PV array, power conditioning unit that converts the DC power to AC power, and the load such as utility grid or local load. Some grid connected systems use battery as storage devices to provide backup power for emergency systems and some important loads during power outages. The generated AC power is injected into the grid and/or utilized by local loads. The block diagram of a grid-connected photovoltaic system is shown in Figure 15.

3.2.1. Power Conditioning Units

The heart of the any PV system is considered to be the Power Conditioning Units (PCUs). PCU is a device used to convert the DC power produced from the PV array to AC power that can be used by the end user. This conversion requires a number of power processing stages that can be classified into single-stage and two-stage systems. In the first, an inverter is used to perform all required control tasks while in the two-stage system, a DC-DC converter is used as power adapter stage preceding the inverter. In this second case, the control tasks are divided accordingly between both converters. Two-stage provides higher control flexibility compared to single-stage systems, but it adds an additional initial cost and reduction in the reliability of the system (14). In order to serve a

wide range of commercial and residential PV applications, different inverter and DC-DC converter topologies are proposed. PCUs are generally designed to perform the functions such as Maximum Power Point Tracker, match the frequency and a phase shift of the current, and other functions that are discussed in the following subsections.

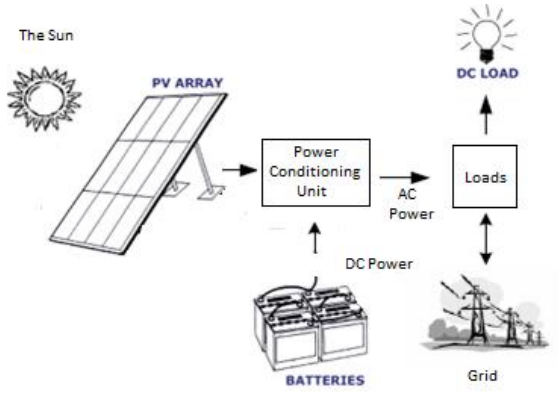

Figure 15: Components of Grid Connected PV System

3.2.2. Maximum Power Point Tracking (MPPT)

In order to maximize the generated power of the PV array at a certain irradiance, temperature, and shading condition, PCUs are designed to track the maximum power point mpp by controlling the output voltage or current of the PV array. Different techniques can be used for this purpose. Partial shading of PV arrays is considered one of the main challenges that face MPPT techniques. Multiple local peaks may exist along the P-V curve, but there is only one global maximum power point that gives the maximum power, as illustrated in Figure 16. In this case, the task of the PCU is to identify and operate at the global MPP. The MPPT attempts to follow the peaks; it is very difficult for MPPT to find the global maximum of these multiple peaks. Research in this field is active and several studies have focused on developing new MPPT techniques and PCU

topologies that can perform this task (14). An optimal MPPT must both follow the global peak of the power curve and avoid the local peaks (15), (12).

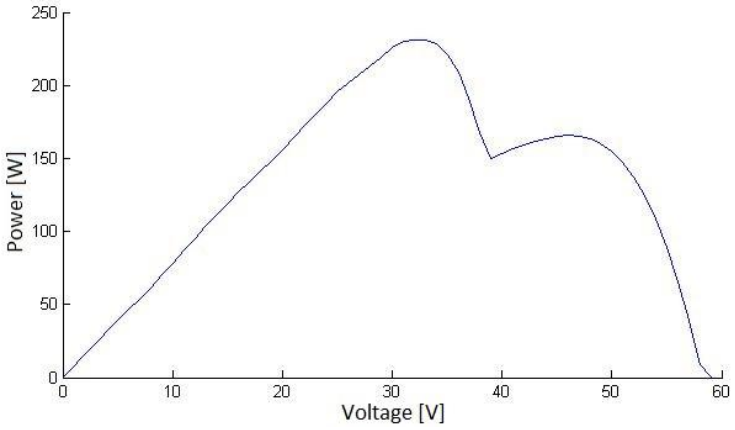

Figure 16: Local and Global Maximum Power Point

3.2.3. Additional Functions

PCU can serve many additional functions besides MPPT. For example, power factor and total harmonic distortion are power quality indicators of PCU output. PCU is responsible to control the sinusoidal current injected into the grid to match the frequency and a phase shift (power factor) of the voltage of the grid at the point of common connection PCC. Moreover, the harmonic of the current should be within the limits specified in the standards (14) (1). Another function is a condition in which a portion of the utility system containing both loads and distributed resources remains energized while isolated from the rest of the utility system is defined as islanding (14). Most of the standards require that PCUs islanding of PV systems should be taken into account to provide safety of the workers (1). One of the important functions of the PCUs is voltage amplification. Usually, the voltage level of PV systems is lower than the voltage of the grid. The output

voltage of the PV system is boosted to match the grid voltage and to decrease the power losses using step-up DC-DC converters or multilevel inverters (7) (13). Additional tasks such as power factor correction, harmonics filtering, reactive power control, and operating with an energy storage device and/or a dispatchable energy source such as diesel generator as an uninterruptible power supply can also be considered as a functions of the PCUs (14).

3.2.4. Energy Storage Devices

The use of energy storage devices with PV systems allows the power generated from these systems to be stored for later use. The installation of storage devices can enhance the performance of PV systems by bridging their power fluctuations, by shifting the time of their peak generation, by supplying critical loads during power outages, and providing reactive power support. There are a variety of storage devices such as batteries, super-capacitors, super-inductors, flywheels, and water pumping (6). These devices vary in their characteristics, method of operation, and accordingly, the tasks that they can perform. Thus, choosing a storage device that can perform the required function efficiently is a preliminary step. Moreover, due to the fact that the majority of storage devices are expensive, it is essential to study the economical value of using these devices (14).

3.3. Connection Topologies of PV Systems

The utility interactive system, the simplest system in terms of its number of components, can be configured with added components to serve its intended purpose and improve efficiency. Different topologies according to the connection of the PV modules with the PCUs are available in the literature. Some of the common topologies are shown in Figure 17.

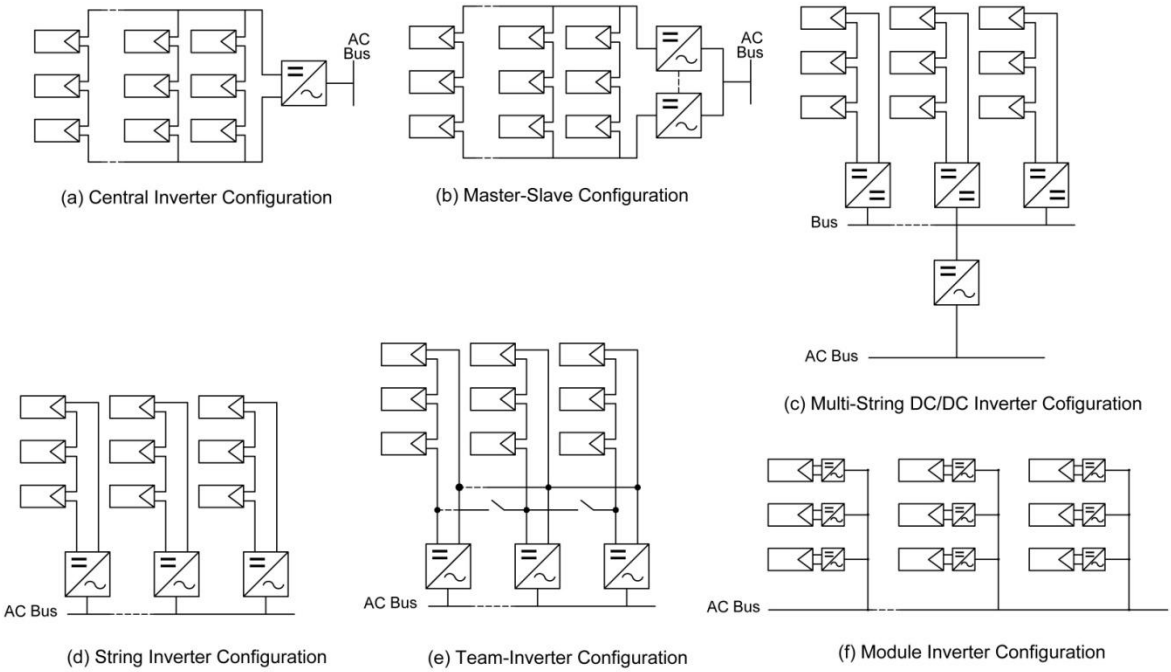

Figure 17: Gird connected PV System Configurations

3.3.1. Centralized Topology

The simplest configuration is the central inverter system, shown in Figure 17 (a), where PV modules are connected to form strings. These strings are connected to a common combiner box then to a central inverter that converts the power from DC to AC to supply the grid. This configuration is usually used for large PV systems up to several megawatts. The main advantage of the central inverter topology is the low cost as compared to other topologies as well as the ease of maintenance of the inverter. However, this topology has low reliability as the failure of the inverter will stop the PV system from operating. Moreover, there is significant power loss in the cases of mismatch between the modules and partial shading, due to the use of one inverter for tracking the maximum power point. This configuration cannot correctly track the maximum power point (MPP) for the whole

array (13), (16), (17). This is because each string has its own MPP according to the operational conditions and shadowing effect.

3.3.2. Master-slave Topology

In order to improve the reliability of the centralized topology, master-slave configuration was developed using a number of parallel inverters that are connected to the array as shown in Figure 17 (b). The required number of active inverters is chosen such that if one inverter fails, the other inverters transform the whole generated power. Moreover, the inverters can be designed to operate according to the irradiance level, where for low irradiance level some of the inverters are shut down (14). This technique extends the lifetime of inverters and the overall efficiency. However, the cost of this topology is higher than that of the centralized topology and electrical mismatching loss due to shading is still a problem PV (14) (7).

3.3.3. Multi-String DC/DC inverter Topology

The Multi DC/DC-central inverter system configuration, shown in Figure 17 (c), improves the performance of the central inverter system during shadowing conditions. In this topology, every string is connected to a DC-DC converter for tracking the maximum power point and voltage boosting. All the DC-DC converters are then connected to a single inverter via a DC bus. This topology combines the advantages of string and centralized topologies as it increases the energy output due to its ability to follow the MPP of each string independently (13), (16), (17) while using a central inverter for reduced cost. However, the losses due to the DC/DC converters are added to the losses of the system.

3.3.4. String-Inverter Topology

In the String Inverter configuration, shown in Figure 17 (d), each string has its own inverter and all inverters operate in parallel to supply the load. The reliability of the system is enhanced. Moreover, the losses due to partial shading are reduced because each string operates at its maximum power point. Additional strings can be easily added to the system to increase its power rating, thus, increasing the flexibility in the design of the PV system. This system increases the system efficiency, but with additional cost due to the increase in the number of inverters (13), (16), (17).

3.3.5. Team Concept Topology

The Team-Inverter configuration, shown in Figure 17 (e), uses controllable switches to connect the parallel string inverters according to the solar insolation (16). The system connects the proper number of strings in parallel to a specific number of parallel inverters, thus maximizing the efficiency of the connected inverters. This topology is used for large PV systems; it combines the string technology with the master-slave concept. During low irradiance conditions, the generated energy from each string in the PV system does not match the optimal working efficiency of the inverters. Therefore, adding more than one string in parallel and connecting them to the optimal number of inverters, the amount of energy will match the optimal working point of the chosen inverter(s). As the irradiance level increases, the PV array is divided into smaller strings to inverters to operate at their rated power.

3.3.6. Module-Inverter Topology

The most recent topology known as the Module-Inverter or (micro-inverter) system, shown in Figure 17 (f), each single module is connected to a separate inverter that can individually operate near the module's MPP. This effectively increases the efficiency of the whole system (13), (18), (16). It has many advantages such as reduction of losses due to partial shading, better monitoring for module failure, and flexibility of array design. However, this topology is suitable only for low power applications (up to 500W) and has relatively high cost (14). Moreover, the lifetime of the inverter is reduced because it is installed in the open air with the PV module, thus increasing its thermal stress.

3.4. PV System Critical Issues

Shading and mismatch losses of PV system are considered very critical problems in the PV systems. Significant reduction in generated power from solar PV arrays occurs when the shading falls across some PV modules, leading to extra losses (19). PV modules are very sensitive to shading. Shading of a single cell within a PV-module, which contains a number of modules connected in series, leads to a reverse bias operation of the cell, which may result in hot-spots and potential breakdown of the shaded cell. As previously discussed in chapter 2, the hot spot in the shaded module is capable of sustaining permanent damage at the cell level. When a small portion of a cell/module/array is shaded, while the remainder is in sunlight, the output falls dramatically. Soft shading sources, a tree branch, roof vent, or chimney, significantly reduce the amount of light reaching the cell(s) of a module. Hard sources are defined as those that stop light from reaching the cell(s), such as a blanket, tree branch, bird dropping or the like, sitting

directly on top of the glass. when one full cell is hard shaded by structure that stops light from reaching the cell(s), the voltage of that module will drop to half of its non shaded value in order to protect itself as shown in Figure 19. If enough cells are hard shaded, the module will not convert any energy and will in fact become a tiny drain of energy on the entire system.

The traditional method to reduce the effect of shading on the modules is to incorporate a bypass diode. In order to prevent damage during shading, current flows via the diode instead of the shaded module.

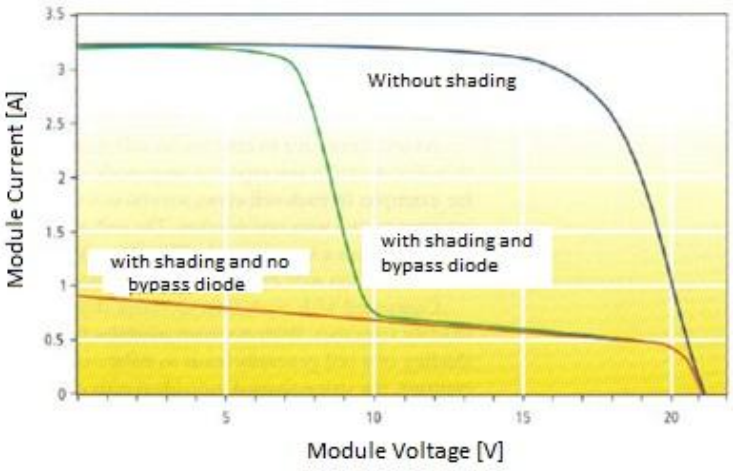

Figure 18: shading and bypass diodes effects (7)

This method usually requires the integration of bypass diodes at the cell or module level, and thus results in extra costs. Furthermore, the power losses of solar PV arrays cannot be completely prevented because there are additional power losses when the current passes though the bypass diodes. Another disadvantage of the bypass diodes is the multiple peaks in the system's output power curve during shading effects (Figure 18) that lead to additional system losses. When the MPP tracker tries to follow the MPP, it will be very

difficult for MPPT to find the optimal maximum of these multiple peaks. Solutions have been proposed to deal with this issue such as the development of more advanced MPPT. However, due to the high cost of these more advanced systems and the complexity of the MPPT control algorithm, the system is still not considered optimal. An optimal MPPT must both follow the global peak of the power curve and avoid the local peaks (15), (12).

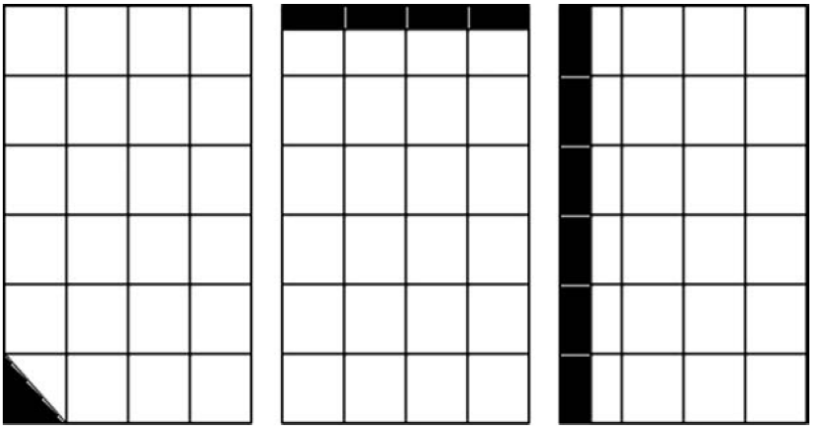

Figure 19: Partial cell shading of a module that will reduce a solar power to 50% (4)

Another important phenomenon in PV field is the mismatching effect of unequal voltage between strings that occur because of dissimilarity between the voltages of the modules in different strings (20), (17). In order to solve this problem, blocking (string) diodes are used in each string to prevent the back feed current between strings. This method is beneficial but also has additional losses that will be added to the PV system losses.

4. Adaptive Photovoltaic System, the Proposed Topologies

4.1. Introduction

Shading can cause many undesired effects. First, real power generated from the solar PV array is much less than nominal power, so that the electrical mismatching losses between the components of PV system increases. Secondly, local hot spots in the shaded part of the solar PV array can damage the solar cells.

There are several approaches that have been used to reduce the effect of shading on a solar PV array output power: 1) bypass diodes are connected across shaded cells to pass the full amount of current while preventing damage to the solar cell. This method usually requires a great number of bypass diodes that are integrated in the solar arrays. The production of solar arrays with bypass diodes is costly. Furthermore, the power losses of solar PV arrays are not completely prevented because additional power losses arise when the current passes through the bypass diodes, 2) in large systems, each of the solar sub-modules can be connected to its own MPPT using DC/DC converters and can individually operate near its own mpp. Thus, the efficiency of the whole system improved, but the method requires a large number of DC/DC converters (equal to the number of PV modules or PV strings), which is called the Multi-String DC/DC inverter configuration, and 3) an alternate research field, which is the focus of this thesis, is to

adaptively reconfigure solar array connections in real time in order to track maximum output power. Traditionally fixed solar PV arrays have hard wired interconnections between their solar cells. These connections are not changed after installation. However, it is possible to continuously rearrange PV modules in series and parallel connections. Research studies have started to develop methods to reconfigure solar cells to improve power output in shaded conditions. Some research focuses on how to manufacture the arrays, and do not propose real-time solution for these abnormal conditions control algorithms. As a result, the methods proposed have unrealistic number of sensors and switches that must use complex control algorithms to determine when it turns the switch ON or OFF. Another research approach uses switching matrixes to reconfigure PV modules according to different operational conditions, thus, optimizing the efficiency of PV system.

This chapter proposes new flexible switching matrixes (FSM) for reconfiguration of solar PV modules in real time under abnormal conditions. As of yet, three different flexible switch matrixes (FSM) that form three different adaptive PV systems are proposed. Each system has special design of FSM that achieves maximum efficiency during shading and module mismatches by reconfiguring the PV modules based on real-time solar insolation, current operational conditions, and maximum efficiency criterion. These adaptive PV topologies are; 1) Adaptive PV Central-inverter configuration, 2) adaptive PV-inverter topology, and 3) Adaptive PV string-inverter configuration. The chapter also includes some illustrations of different operational conditions and the controller logic.

4.2. Reconfiguration and Photovoltaic System

Different methods are used to achieve reconfigurations at the cell, module, and array levels. Dissimilarity in the output of PV modules can occur in the PV array. Dissimilarities may arises from shading across some modules, and manufacturing differences in the I-V characteristics of each module. Since each PV module has a different MMP, the dissimilarity results in the reduction of the harvested power (20). In other words, the PV system interface, connections, and the configuration of the components are vital to achieving a system performance adequate enough to encourage more widespread PV installation. The performance of the PV system not only depends on operational conditions such as shadowing, high temperatures, or the degradation of the electrical characteristics of damaged panels, but it is also strongly dependent on the PV system configuration.

Much of the current research in this field is focusing on improving the efficiency of PV cells through the development of new semiconductor structures that give better behavior. Researchers are looking to improve the performance of PV systems by tracking the optimal operational conditions and configuration topologies, and implementing power electronic devices that improve efficiency. In (20), a modular DC/DC converter topology is proposed to reduce the number of DC/DC components that track the mpp used in stand-alone PV systems. This topology requires all PV modules to work in parallel which may not be applicable for large scale installations. In (19), a reconfiguration at the cell level is discussed to address the shadowing effect and increase the output power through the addition of external reconfigurable cells. In (21), (18), dissimilar cells are matched through reconfiguration to improve the system efficiency. Improvements to the

system are accomplished through the reconfiguration of a large number of switches and sensors at the cell level. In (22), an Electrical Array Reconfiguration (EAR) is proposed at the module level using a switching matrix that can change the position of the modules to achieve better matching between similarly illuminated PV modules. The system is used to maximize the available DC power by matching modules that have similar operational conditions**.** In (23), reconfiguration is proposed for an electric vehicle to increase its power output and operate the load at the desired conditions to improve the load efficiency. During acceleration, for example, the engine requiring additional torque is supplied by reconfiguring the PV in parallel to increase the current output. In (24), the optimum switching points for the array reconfiguration controller is discussed according to the insolation conditions.

4.3. Adaptive PV Systems and Flexible Switching Matrix [FSM]

Adaptive photovoltaic systems are based on novel flexible switch matrixes [FSM]. The controllable elements are switches that can be controlled for on/off operation to provide features for connecting adjacent devices adaptively including parallel, series, or parallel/series connection and selective device isolation. Examples of switches include relays, contactors, bulk and integrated NMOS, PMOS and CMOS transistors, and MEMS switches, depending on the particular technology and application. The internal terminals are used to connect the equivalent device configuration to the external terminals. Finally, the external terminals are used to connect the topology to the external systems. The ports are interchangeable depending on the specific devices used in the topology and what is being implemented. In the following subsections, each FSM has additional switches and

buses at each port to connect the ports to the internal terminals according to the required function of the system.

4.3.1. Adaptive PV Central-Inverter Configuration

A novel Adaptive photovoltaic system based on a modified FSM that establishes an interface between the PV modules/strings and the power conditioning units is proposed for utility interactive systems. This configuration is called the adaptive PV central-inverter configuration. The proposed configuration offers a flexible connection to rearrange the PV modules according to the operational conditions. This topology is incorporated into a fully adaptive utility interactive system as shown in the simplified block diagram in Figure 20. The system consists of five major components: The PV modules, FSM, the inverter, the DC/DC converter, and the controller. Using this adaptive system, the configuration that most efficiently extracts the maximum potential power from the PV is selected. For example, if shadowing occurs across some modules, the matrix will reconfigure the system and utilize the DC/DC converter to achieve the best configuration. Each module has a specific number of switches.

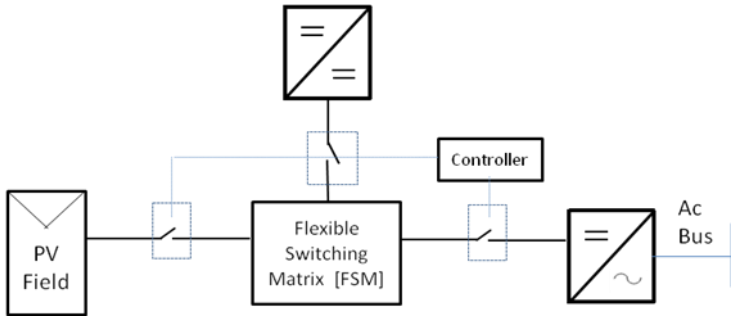

Figure 20: The proposed topology

4.3.1.1. The Flexible Switching Matrix

The special FSM topology is shown in Figure 21. It consists of switches and buses. The buses connect the terminals of the matrix to the proper device while the switches are responsible for the organization of the PV modules in the matrix. The matrix sorts the modules into two categories. The first is the main PV string (MPV), which connects PV modules in series to form a string. The other is the sub PV string (SPV), which forms a sub string that consists of the PV modules that don't meet the required number to form an MPV.

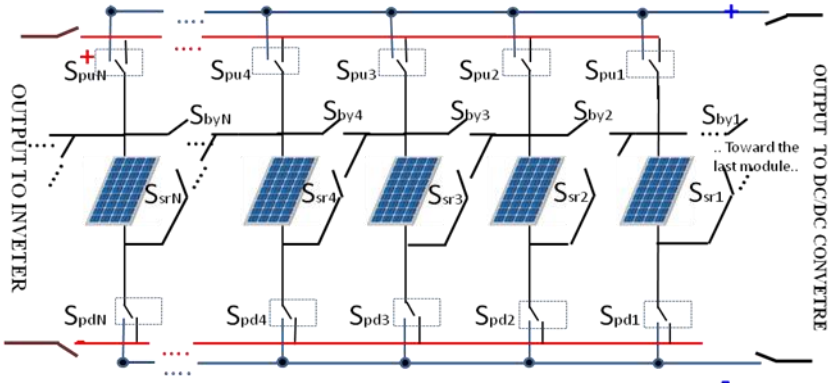

Figure 21: The proposed FSM topology with PV Modules (25)

The switches in the modified FSM are categorized according to their function. The (S_{sr}) are switches used to achieve the series connection between the PV modules. The series connection may happen between adjacent/nonadjacent modules, that is, for example, between the first and the third modules. This connection is achieved using switch S_{by2} in addition to switch S_{sr1}. The (S_{by}) are switches that allow modules to be removed (bypassed) from the configuration. In the last example, the connection between the first and the third module is achieved using (S_{by2}) bypassing the second module. The (S_{pu}) are

switches that connect the positive terminal of the module to the positive buses. Activating any of the switches will establish the end of the string. The (S_{pd}) are switches that connect the negative terminal of the module to the negative buses. Closing (activating) any of the switches will determine the beginning of the string. Each of these switches can be connected to the inverter bus position that has no prefix in the switch symbol (i.e. S_{pd9}) or they can be connected to DC/DC converter bus by switches position that has DC/DC suffix (e.g. $S_{pd9DC/DC}$).

Two different types of buses are used to connect PV modules to the inverters. The first type is the string-buses that connect the PV strings to the central inverter. The second type is the DC/DC-buses that connect the SPV modules to the DC/DC converter. For example, under normal conditions each string will be connected to a central inverter through a string-bus and due to the normal conditional no additional MPV string can be formed.

The number of switches in the matrix depends on the number of modules in the PV array. Each module requires four switches in order to achieve the adaptive system. Each bus requires two switches to connect the MPVs and SPV to the inverter and the DC/DC converter; hence:

$$N_{SW} = 4(N_{mod}) + 2(N_{DC}) + 2(N_{inv}) \qquad (11)$$

Where N_{sw}: is the number of switches required for the adaptive PV system.

N_{mod}: is the number of modules in the PV array.

$2(N_{DC})$ and $2(N_{inv})$: are for the inverter and DC/DC converter switches.

4.3.1.2. Adaptive PV Central-Inverter Operation

A 9-module system is used to illustrate the adaptive operation of the adaptive PV central-inverter system. The system consists of three strings with three modules in each string connected by 40 controllable switches. The system also consists of four buses; with two string-buses connecting the MPV strings to the central inverters, and the two remaining buses connect the SPV modules to the DC/DC converter. An illustrative block diagram of the system is shown in Figure 22. The examples that follow focus on shading issues. The adaptive nature of the topology also applies to non matched modules and faulty modules; reconfiguration can take place to optimize the efficiency of the overall system operation.

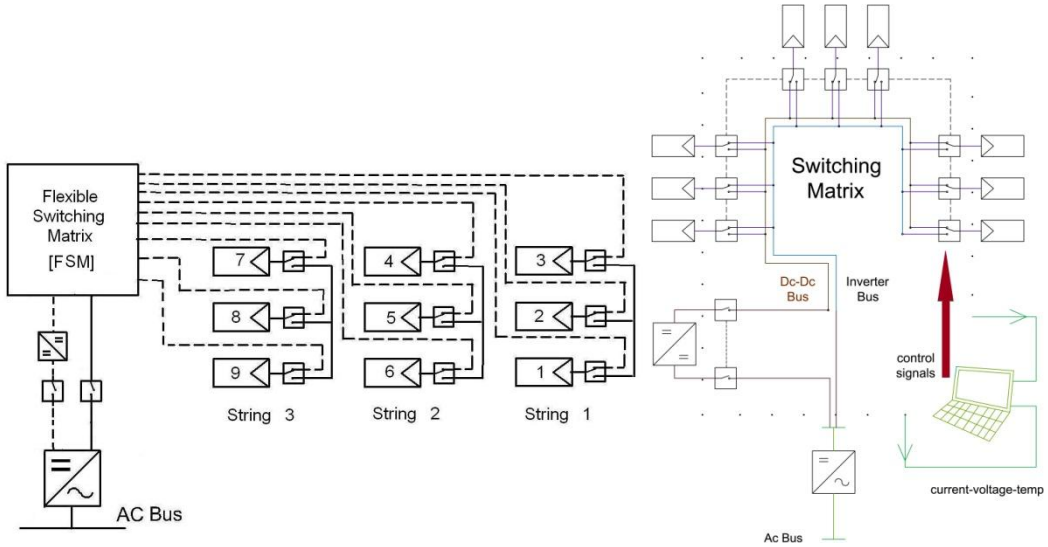

(a) one line diagram layout (b) Detailed layout including the controller

Figure 22: Adaptive PV central-inverter configuration layouts (25)

(1) Normal Operation

This operation case occurs when all PV modules are active (generating nominal power). The matrix will activate the series switches S_{sr1}, and S_{sr2} to complete the required number of modules in series in the first string, and this process will be applied to the second string by activating S_{sr4} and S_{sr5}. In order to connect the PV strings to the inverters, the matrix inactivates S_{sr9}, S_{sr3}, and S_{sr6}. The parallel switches S_{pd1} and S_{pu3} will also be activated to connect the first MPV string to the first string-bus. Switches S_{pd4}, S_{pu6} will be activated to connect the second MPV string to the second string-bus. In this case, the bypass switches (S_{by}) will be inactivated. All PV strings are of the MPV string category and match the distribution of the traditional central inverter configuration shown in Figure 17 (a). The DC/DC converter will not be used because no SPV string can be formed in the matrix.

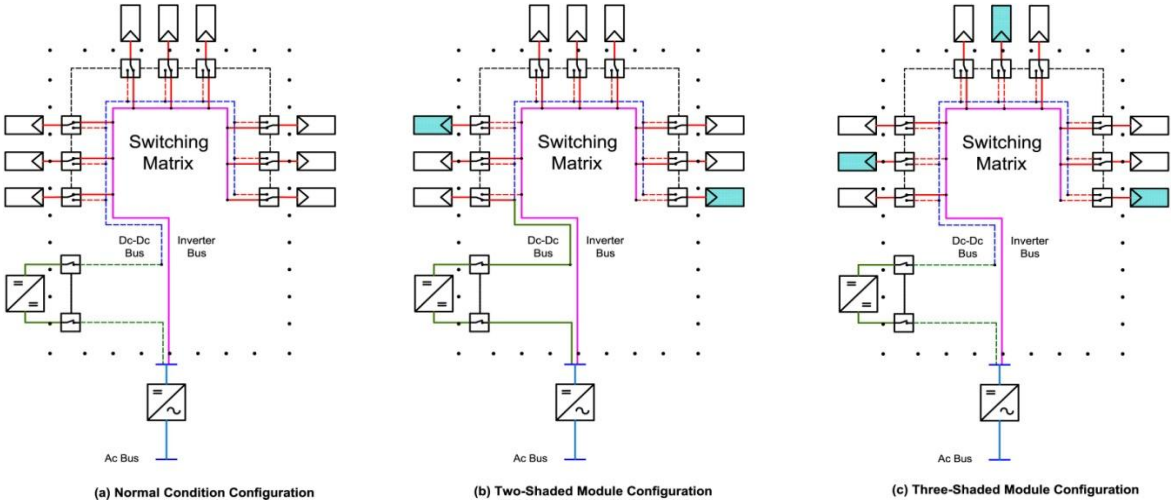

Figure 23: Adaptive PV central-inverter configuration operation in various conditions (25)

(2) Two Shaded Modules

Modules # 1 and #7 will be considered shaded for this example. The series switches S_{sr1} and S_{sr7} of the shaded modules will be deactivated to isolate these shaded modules. At the same time, the bypass switches S_{by1} and S_{by7} are activated to connect the adjacent modules to the shaded module, modules #6 and #8 in this case. If the matrix does not have the number of modules in series in the string completed, the procedure will continue in order to achieve the required number of modules in the PV string to form the MPV string. In this case, the first string will begin with PV module number 2.

The parallel switches will be activated when the MPV string is perfectly formed. Then, switches S_{pu2} and S_{pd4} will be activated in order to connect the first MPV string to the string-bus and then to the central inverter. This process will be applied to the second string by activating S_{pu5} and S_{pd8}. In this case, the array has one remaining module that does not meet the requirement to build a string, and it can also generate energy. The matrix will consider this module as an SPV string and will connect it to the DC/DC-bus and DC/DC converter and finally to the central inverter using switches $S_{pu9DC/DC}$ and $S_{pd9DC/DC}$.

(3) Three Shaded Modules

Modules # 1, #5, and #8 will be considered shaded for this example. The series switches S_{sr1}, S_{sr5}, and S_{sr8} of the shaded modules will be deactivated. The bypass switches, $S_{by1,}$ $S_{by5,}$ and S_{by8} will be activated to form MPV strings without shaded modules. The nonadjacent modules can be connected in series using S_{by5} and $S_{by8.}$ Modules # 7 and #9 will be connected in series for example. The parallel switches will be activated when the matrix forms an MPV string. Switches S_{pu2}, S_{pd4} of the first string and S_{pu6}, S_{pd9} of the

second string will be alternated. In this case, the array doesn't have any remaining modules that meet the requirements of the neither MPV string nor SPV string. Therefore, since no SPV string can be formed in the matrix, the DC/DC converter will not be used.

4.3.1.3. Control System for Adaptive PV Central-Inverter Configuration

The control algorithm for adaptive PV central-inverter configuration is illustrated by the flow chart in Figure 24. The operation of the system contains two functions represented as loops in Figure 24. The left loop is responsible for identifying the condition of each PV module. This can be done by measuring its parameters (current, voltage, temperature) of each PV module and schedule them in matrix in such a way that indicate the number of the module in the FSM and its status (shaded or active) (i.e. $M_{[number, status]}$). The diamond shapes represent the examination function while the square blocks represent the command (i.e. close the switches or inactivate it). Under normal operating conditions, the system will configure the modules in the normal MPV strings configuration and no SPV string will be created inside the matrix. In shading/fault operation, the system will isolate the affected module(s) and reconfigure the remaining modules to form MPV and SPV strings as required for optimal operation. In order to reconfiguring the remaining modules, each module is examined with respect to each MPV. Pointers are used to identify the location of each module in the string (i.e. $M_{[number, status]}$).

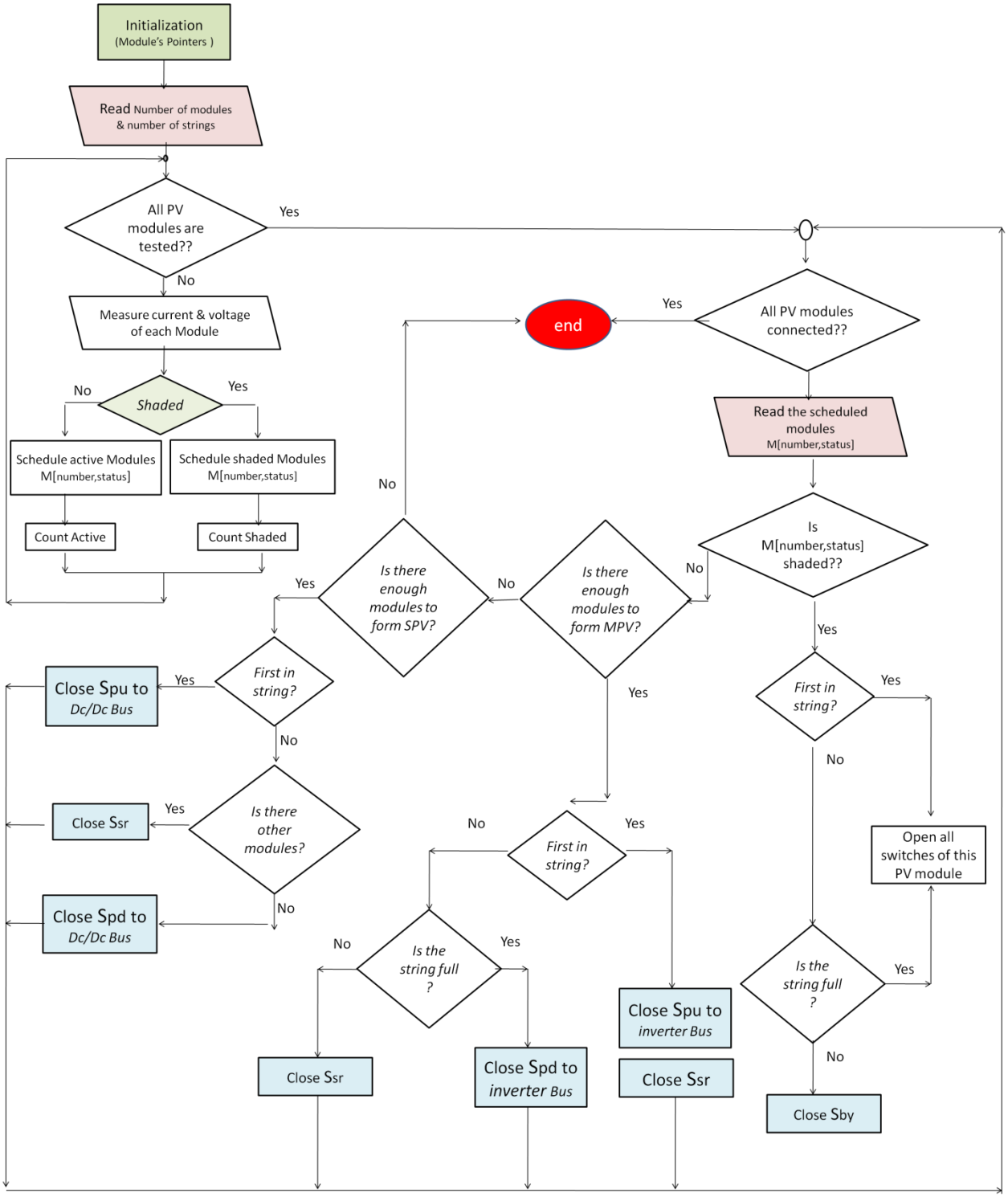

Figure 24: Adaptive PV central-inverter control flow chart

For example, when the first module is not-shaded, it is scheduled as $M_{[1, active]}$ and later the second loop (the right loop in the Figure 24) will add it to form the MPV string. The second loop starts when the controller examines the next module to determine the connection order. The controller will also track the number of modules in each MPV string. If the MPV string is incomplete, the controller will connect the next active PV module in series to other modules already located in the same MPV string. Once the MPV string is complete (the pointers gives a signal that the module is at the end of string), no more MPV strings can be formed (because the remaining number of active modules are less than the capacity of the MPV string), and the controller will arrange the other modules in the SPV string. All connections can be done using the appropriate switches order which is determined by the controller. The logic of the controller is illustrated for this point of the research. The actual controller design and implementation will be considered in future work.

4.3.1.4. Advantages of the Proposed System

The proposed adaptive PV central-inverter configuration has the ability to overcome the shading and mismatch limitations of the traditional PV system and to provide for fault tolerant design, the mismatching effects of unequal voltage between strings. In the proposed adaptive PV central-inverter configuration, shaded modules can be eliminated by isolating them from the affected strings using the flexible connections between the modules. This process is achieved using the FSM and the control algorithm to select the optimum configuration after removing the shaded modules. Using this approach, the electrical losses caused by bypass diodes and blocking diodes are further minimized.

Furthermore, the inherent multiple peaks phenomenon is resolved so that a simple MPPT can be used. Results show improvements in the characteristics of the output power curve.

4.3.2. An Adaptive Photovoltaic-Inverter Topology

A simplified block diagram of the proposed adaptive system layout is shown in Figure 25. The proposed approach offers a flexible connection to rearrange the solar modules according to operating condition. Using a switching matrix topology and suitable inverters configuration, the system will extract the maximum potential power efficiently from the PV array by adapting to the best operating conditions. For example, in low radiation conditions, the matrix will reconfigure the system and utilize the micro/string inverters to achieve the best operating conditions based on real time conditions. The system consists of five major components: the string-PV modules, the micro-PV modules, the switching matrix, the micro inverters, and the string inverters.

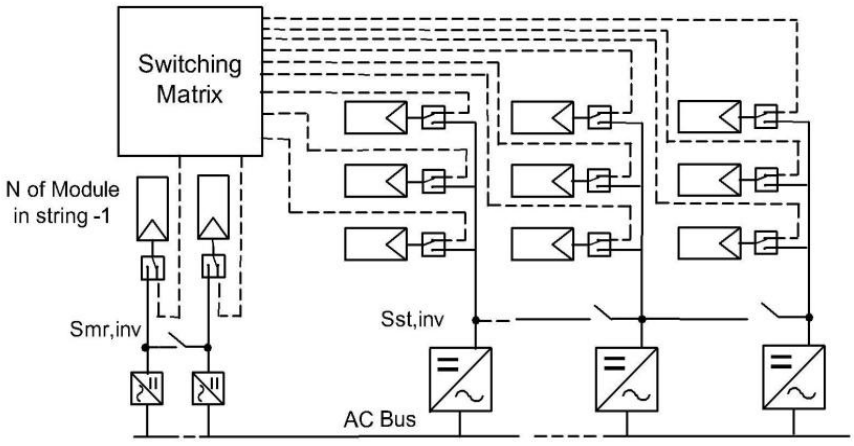

Figure 25: Adaptive PV-inverter layout

4.3.2.1. The Switching Matrix

The matrix topology that reconfigures the connections between PV modules is similar to the FSM that was proposed in Adaptive PV central-inverter configuration. The only difference is that each PV module is connected to a bus, which has two ports, thus connecting the modules either to micro-inverter or to string inverter. In this case, all PV modules, string-modules, micro-modules, switches, and buses are the components of the switching matrix. For example, in the normal condition each string will be connected to string-inverter through a string-bus port and each of the micro-PV modules will be connected to the micro-inverter through micro-bus port.

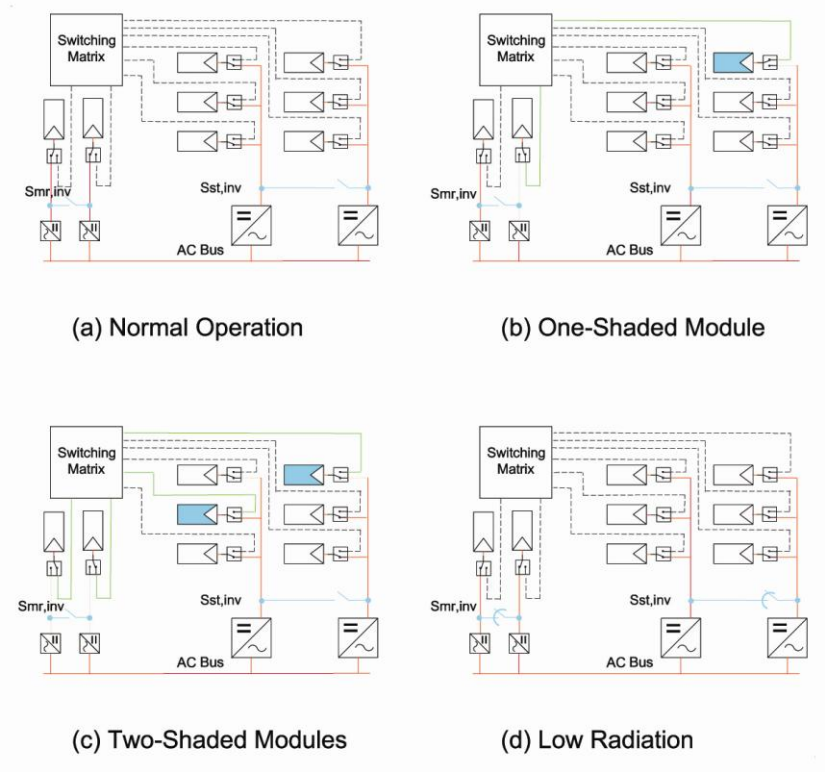

Figure 26: Different operational conditions for adaptive PV-inverter topology

For an 8-module PV array, 42 switches are required. Four buses are used in this system; two string-buses are used to connect two PV strings to the string-inverters; the other two buses are micro-buses used to connect two micro-PV modules to micro-inverters. These buses are considered the point of common connection of the PV modules to supply the inverter.

The number of switches in the matrix depends on the number of modules in the PV array. Each module requires four switches in order to achieve the adaptive system. Each bus requires two switches to connect the PVs to the inverter and two switches between the PV strings/micro-PV modules; hence:

$$N_{SW} = 4(N_{mod}) + 2(N_{st,inv}) + 2(N_{mr,inv}) + (N_{st,inv} - 1) + (N_{mr,inv} - 1) \qquad (12)$$

Where:

N_{sw}: is the total number of switches,

N_{mod}: is the number of modules in PV array,

$N_{st,inv}$ and $N_{mr,inv}$ are for the number of string-inverter and micro-inverter switches, respectively.

4.3.2.2. The Matrix Operation

In order to explain the matrix operation, illustration 1, 2, 3 and 4 are provided. The illustrations are built according to the PV array shown in Figure 26 with three strings and three modules in each string.

(1) Illustration 1 (Normal operation)

The desired configuration is shown in Figure 26 (a), all modules are active. The matrix will activate the series switches S_{sr2}, and S_{sr3} to complete the required number of modules in series in the first string, and this process will be applied to the second string by activating S_{sr5} and S_{sr6}. In order to connect the PV strings to the inverters, the matrix inactivates S_{sr1}, S_{sr4}, and S_{sr7}. The parallel switches S_{pd1}, S_{pu3} will also be activated to connect the first PV string to the first string-bus. Switches S_{pd4}, S_{pu6} will be activated so that the second PV string connects to the second string-bus. In this case, the bypass switches (S_{by}) will be inactivated. Each micro-PV module will be separately connected to each micro-inverter via a micro-bus.

(2) Illustration 2 (One shaded modules)

One shaded module is examined. The desired configuration is shown in Figure 26 (b). The series switches S_{sr1} of the shaded module will be opened. In this case, the PV array has two modules that are not enough to build another full string. That means the matrix will consider bring one of the micro-PV modules and will connect it to the string. In this case, the string is completed and the rest of modules will be connected to micro-buses then to the micro-inverters.

(3) Illustration 3 (Two shaded modules)

Two shaded modules from different strings are examined. The desired configuration is shown in Figure 26 (c). The series switches S_{sr1} and S_{sr6} of the shaded modules will be inactivated. At the same time, the bypass switches S_{by1} and S_{by5} will be activated to connect the modules which are nonadjacent in series. For example, modules number 5 and 7. If the matrix does not have the number of modules in series in the string

completed, the procedure will continue in order to achieve the required number of modules in the PV string. In this case, the first string will start with module number 2.

The parallel switches will be activated when the number of modules in series in the string is matching the required number of modules in the string. Then, switches S_{pd2} and S_{pu4} will be activated in order to connect the first string to the string-bus then to the first string-inverter and this process will be applied to the second string by activating S_{pd5} and S_{pu7}. In this case, the array doesn't have any remaining module that meets the requirement to build a full string or micro.

(4) Illustration 4 (low radiation)

The case of low radiation across PV modules is examined. The desired configuration is shown in Figure 26 (d). The matrix will arrange the modules exactly as the configuration during normal operating condition (Illustration 1). The only difference will be the connection to the inverters. Switches $S_{st,inv1}$ and $S_{st,inv2}$ will be activated to connect the string-buses in parallel to only one string inverter. This process will also be applied to the micro-buses by activating $S_{mr,inv1}$ and $S_{mr,inv2}$ to connect the micro strings in parallel.

4.3.2.3. Control System

The reconfiguration strategy is based on the fact that the switching matrix has to rearrange the active PV modules in series into multiple strings to meet the required voltage level of each PV string. The control algorithm of the switching matrix is illustrated by the flow chart in Figure 27. The controller does the following functions: first of all, identify module conditions based on system parameters. If full-shading/fault exists, then a) disconnect the shaded modules b) reconfigure the active modules into strings and

micro-strings. If shading does not exist, then the matrix will configure the modules in the normal configuration.

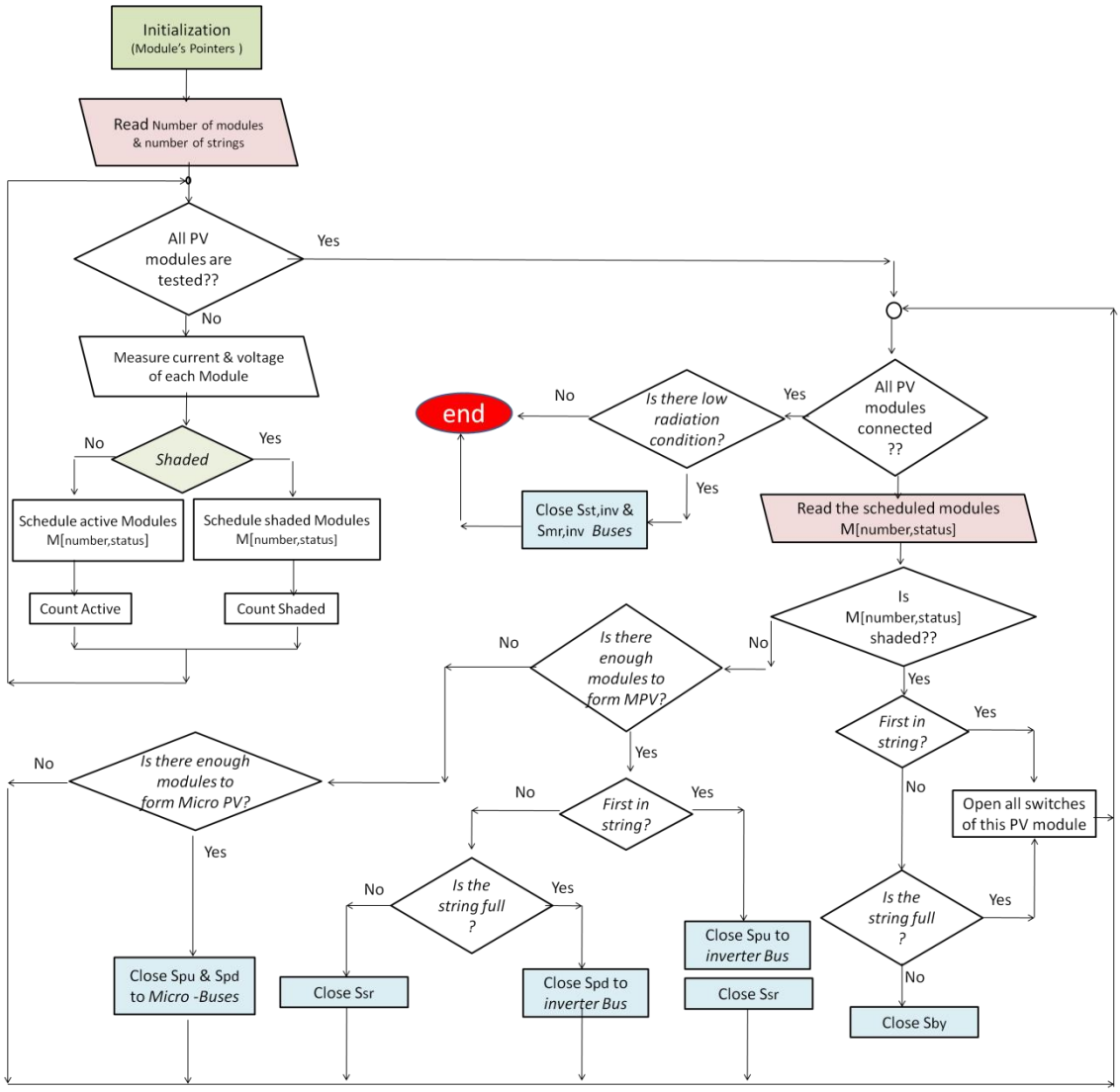

Figure 27: The Control flow chart for Adaptive PV-inverter topology

The controller will arrange the modules in strings and micro strings. To accomplish this, each module is examined to determine whether it is shaded or not and also if it is located in the beginning of the string, in the end of the string, or in the middle of the string. In order to know the location of the modules in the sting, pointers are used to locate them

accurately. For example, In case of non-shaded module, the controller will put the active module in the string. When the controller examines the next module, the controller will also examine the string whether the string is full or not. If the string is not full, the controller will connect the module in series to the other modules that are in the same string; Once the string becomes full (the pointers gives a signal that this module is at the end of string), the controller will arrange the other modules in micro-strings. In case of low radiation, the controller will exactly arrange the modules as the case of normal condition, which consists of strings and micro strings. The controller will then connect the strings in parallel to the suitable number of string-inverters and also will connect the micro-strings in parallel to micro-inverters.

4.3.3. Adaptive PV String-Inverter Configuration

Similar to all previous proposed configurations, this topology can be incorporated into string inverter and micro-inverter PV system configurations to form a new adaptive PV system. The proposed configuration reduces the number of required switches required in previous proposed topologies. This configuration is considered to be the revised and last version of the adaptive system in this research. Figure 28 shows the layout of the system.

4.3.3.1. Adaptive PV String-Inverter System Components

In the Adaptive PV string-Inverter topology, the PV array consists of three subsystems. The first is a flexible string (FST), the second subsystem consists of flexible PV module (FPVM) that form an aid string (AST), and the third is bus structure. Each FST uses four switches while each FPVM uses three switches. The buses connect the strings and the

modules together to the string/micro inverters through switches. Unlike the previous proposed topologies, the system includes only one adaptive string (the AST) that can be used to overcome the shading problems occur across the other strings. Figure 29 shows the all components of the system including the switching matrix.

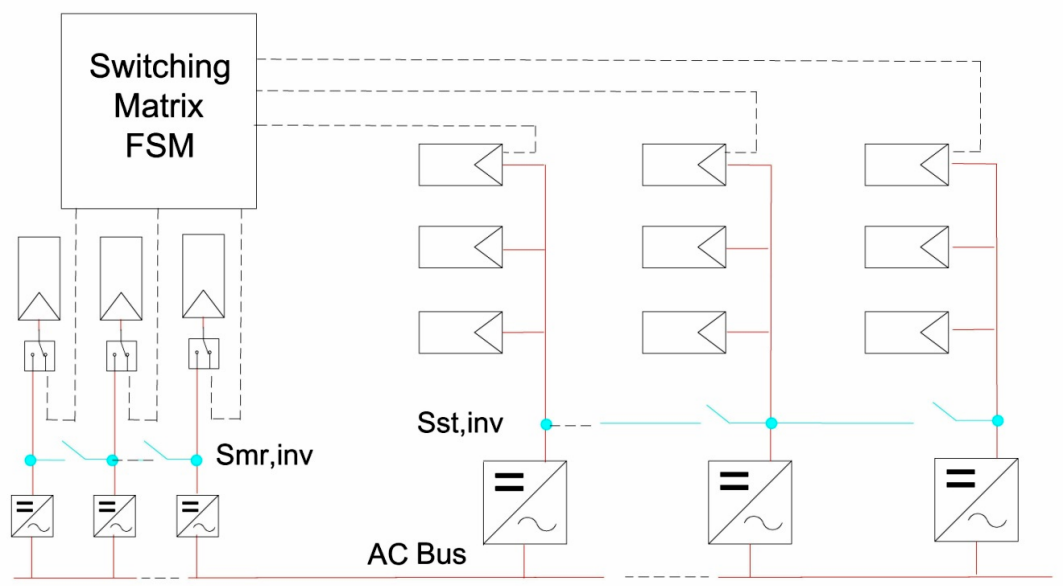

Figure 28: Layout of Adaptive PV string-inverter configuration

As of yet, the performance of the array is very effective and close to the optimal desired performance as will be discusses later in chapter 5. Moreover, any existing system can be converted to adaptive system by changing one sting to adaptive string (AST), including micro-inverters, and by adding some switches to the fixed string to convert it to be FST. This configuration can be applied to string-inverter configuration incorporated with micro-inverter configuration.

The number of switches required for the switching matrix is calculated by this equation:

$$N_{switches} = N_{FST} \times 6 + N_{FPVM} \times 3 + (N_{FST} - 1) + (N_{FPVM} - 1) \qquad (13)$$

Where:

$N_{switches}$: is the total number of required switches in the system.

N_{FST} : is the number of Flexible strings in the system.

N_{PVPM} : is the number of Flexible PV modules in the aid string.

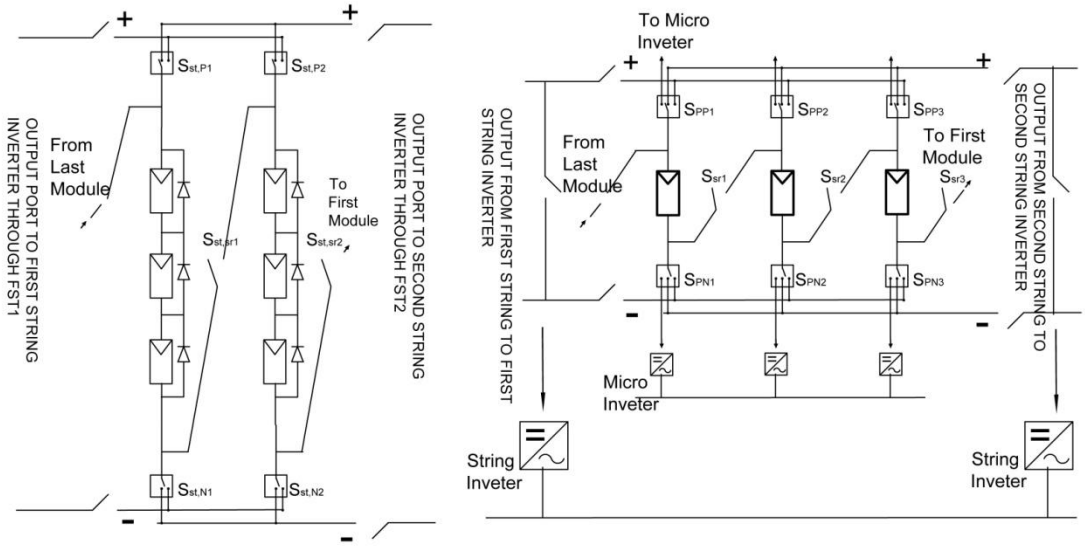

Figure 29: The Switching Matrix And Components Of the Adaptive PV string-inverter System

4.3.3.2. Adaptive PV String-Inverter Configuration Operation

Figure 30 illustrates different operational conditions for Adaptive PV string-inverter configuration and

Figure 31 illustrates the flow chart of the control logic that is designed to accomplish the required configurations. Under normal operational conditions Figure 30 (a), the aid string (AST) works in parallel with other flexible string as a micro inverter configuration system. Each FPVM is connected to a micro inverter and the FST is connected to a string inverter. At the terminals of the string and in order to determine the configuration of the

modules, each FST should have current and voltage sensors while each FPVM should have I, and V sensors. As can be seen, the total number of sensors in this topology is less than the required number of sensors for the previous two topologies. In case of low radiation (Figure 30(b)), the parallel switches will be activated to connect the strings in parallel. This parallel connection is helpful to increase the input energy of the string/micro inverter as shown in Figure 30 (b).

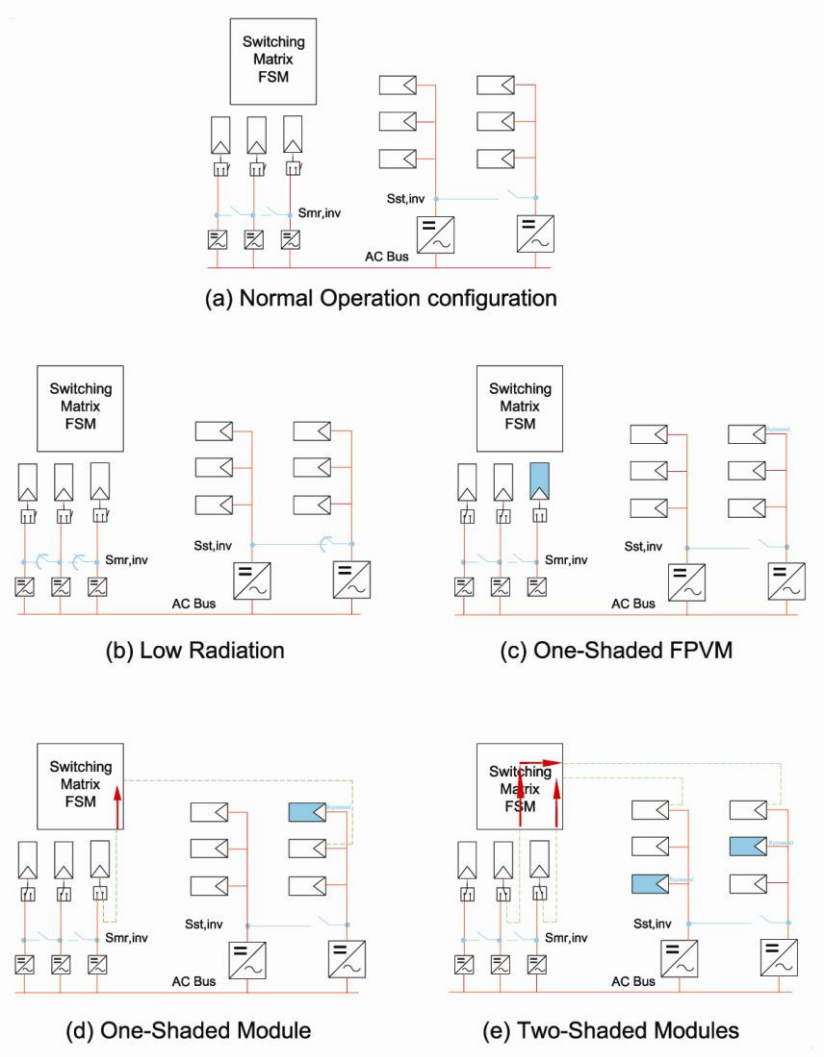

Figure 30: Different operation conditions for Adaptive PV string-inverter configuration

In case shading occurs across FPVMs as shown in Figure 30 (c), the module's sensors will detect the shaded modules and the controller will disconnect it from the matrix. The remaining illuminated FPVM modules in the AST can work separately through micro inverters. In other words, disconnecting the shaded FPVM does not affect the operation of the illuminated FPVM.

In case shading occurs across some modules of FST, the sensors of the shaded string, that are located at the terminals of each FST, will detect a voltage drop, which is the result of using a bypass diode. These sensors will not be able to determine exactly which modules are shaded. However, the controller can calculate the exact number of missing modules in that string according to voltage deviation from the nominal voltage of the normal string. Two cases should be discussed. First, if shading occurs across modules of the same string as shown in Figure 30 (d), FPVMs will be connected to this particular shaded string. Second, if shading falls across modules of different strings as depicting by Figure 30 (e), the AST string will be disassembled into FPVMs and these FPVMs will be distributed across the shaded FSTs. FPVMs will be connected in series to the shaded string to compensate the voltage drop. If there are some unused FPVMs, the controller will connect them to micro inverters. In this case, the system may still have the problem of multiple peaks in P-V curves, but shading problem can be fixed with less number of switches and less number of I, V sensors.

In cases of soft shading, the resultant voltage of the FST will increase as the number of modules in the strings increases. The inverters and switches should be carefully designed to avoid overvoltage problems. Result and analysis of this topology will be discussed in chapter 5.

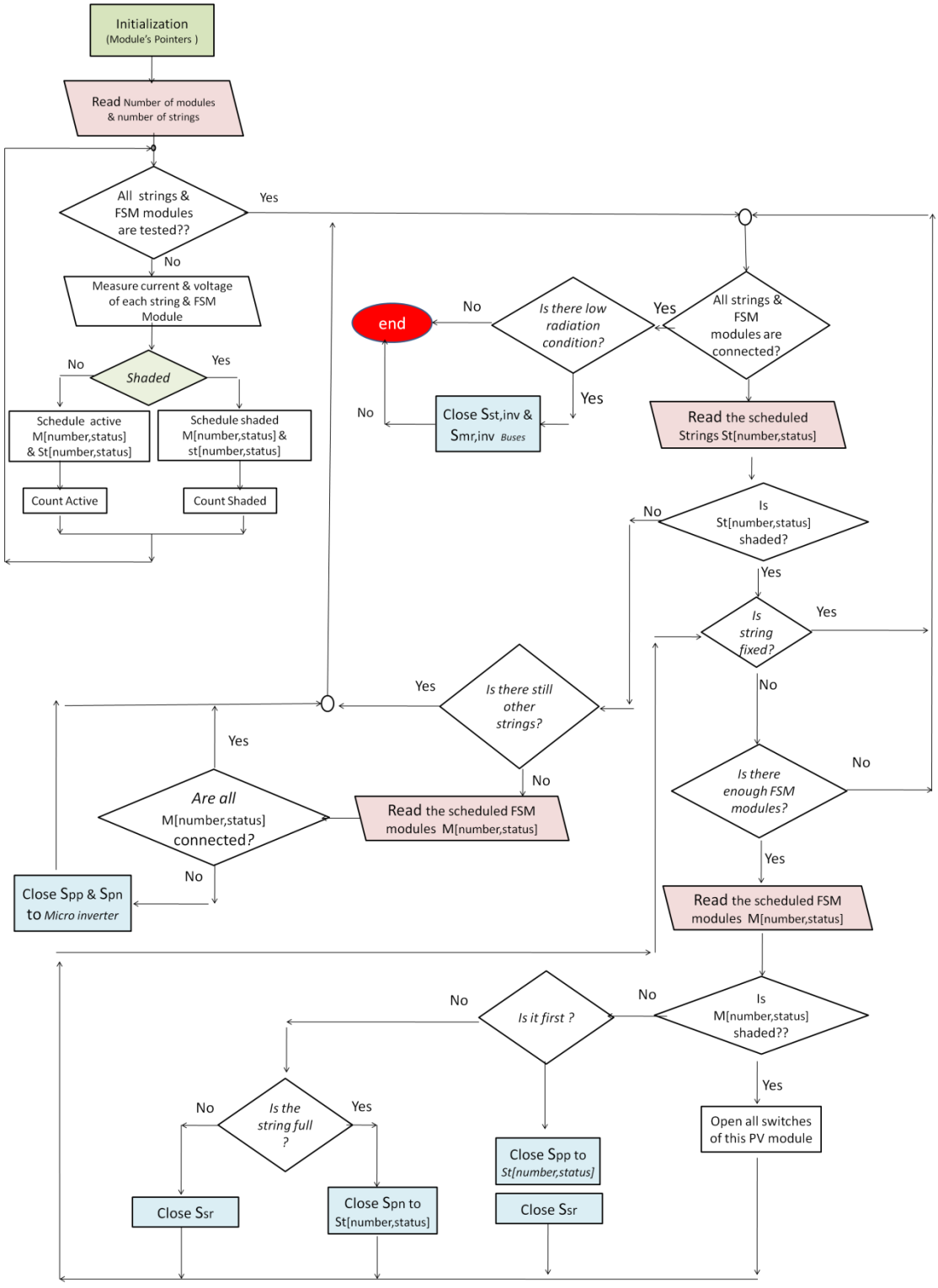

Figure 31: Adaptive PV string-inverter configuration control flow chart

4.3.3.3. Optimizing the Configurations of Adaptive PV string-inverter configuration

Table 1 shows different possible configurations for Adaptive PV string-inverter configuration according to number of modules per string and the number of strings that form a PV system. For example, 40-module PV array can be formed as: 1) total four strings using 59 switches, three are FST and the other is AST, 10 modules each string; or 2) as total five strings using 58 switches, four FST and one AST , 8 modules each string; or 3) as total eight strings using 67 switches, seven FST and one AST , 5 modules each string. As can be seen, the more the number of modules, the more the configurations. Furthermore, the number of witches may be inefficiently chosen. Figure 32 is developed to help determine the optimal configuration according to system per unit [p.u.] and number of switches. As can be seen, each curve represents a configuration. Interconnections between the curves illustrate the points which have the same system size at the X-axis and number of switches at Y-axis.

Table 1: Different Possible configurations for Adaptive PV string-inverter configuration

number of FST (number of string inverters)	1		2		3		4		5		6		7	
modules per st(number of micro-inverters)	number of switches	system size [p.u.]	number of switches	system size [p.u.]	number of switches	system size [p.u.]	number of switches	system size [p.u.]	number of switches	system size [p.u.]	number of switches	system size [p.u.]	number of switches	system size [p.u.]
2	13	4	20	6	27	8	34	10	41	12	48	14	55	16
3	17	6	24	9	31	12	38	15	45	18	52	21	59	24
4	21	8	28	12	35	16	42	20	49	24	56	28	63	32
5	25	10	32	15	39	20	46	25	53	30	60	35	67	40
6	29	12	36	18	43	24	50	30	57	36	64	42	71	48
7	33	14	40	21	47	28	54	35	61	42	68	49	75	56
8	37	16	44	24	51	32	58	40	65	48	72	56	79	64
9	41	18	48	27	55	36	62	45	69	54	76	63	83	72
10	45	20	52	30	59	40	66	50	73	60	80	70	87	80
11	49	22	56	33	63	44	70	55	77	66	84	77	91	88
12	53	24	60	36	67	48	74	60	81	72	88	84	95	96
13	57	26	64	39	71	52	78	65	85	78	92	91	99	104
14	61	28	68	42	75	56	82	70	89	84	96	98	103	112
15	65	30	72	45	79	60	86	75	93	90	100	105	107	120
16	69	32	76	48	83	64	90	80	97	96	104	112	111	128
17	73	34	80	51	87	68	94	85	101	102	108	119	115	136
18	77	36	84	54	91	72	98	90	105	108	112	126	119	144
19	81	38	88	57	95	76	102	95	109	114	116	133	123	152
20	85	40	92	60	99	80	106	100	113	120	120	140	127	160

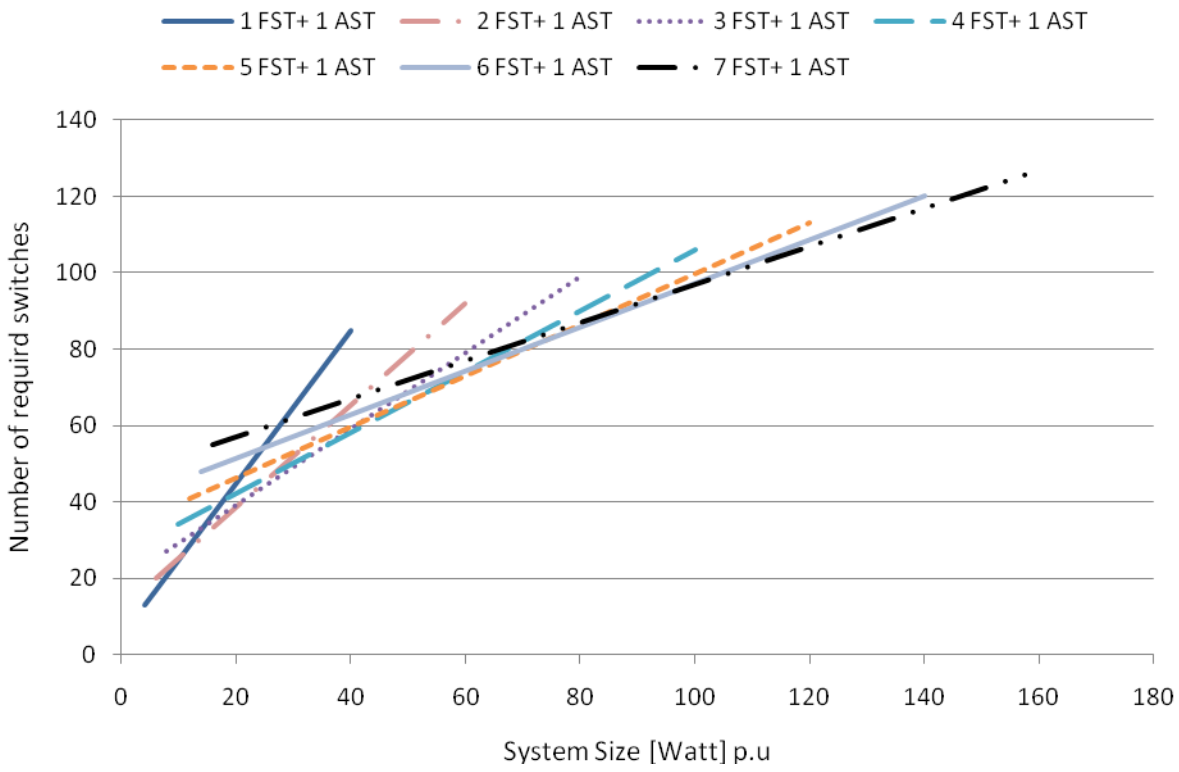

Figure 32: Configuration Optimaization chart according to system per unit [p.u.] and number of switches

4.3.4. Cost analysis

PV modules are the most expensive part of the solar system; however, the cost of the additional switches should also be taken into account to have clear idea about the total system cost. After searching for suitable controllable switches, the cost is $5 for an average multipurpose relay that can withstand wide range of voltages and currents (SNAPTRACK™ 10A SPDT Relays). When installing Adaptive system, each configuration uses different number of switches to achieve the reconfiguration. For a rough estimation of the additional cost, 100 W PV module is selected for this study. The average cost of the PV is $4 per Watt (3). That leads to $400 per PV module. For Adaptive PV Central-inverter configuration, the total number of switches per module

according to equation #11 is 4 switches and 2 switches per PCU. Adaptive PV-inverter topology, the total number of switches per module according to equation #12 is 4 switches, 2 switches per PCU, and more parallel switches depending on the system size.

Adaptive PV string-inverter configuration, the total number of switches per flexible PV module according to equation #13 is 3 switches, 6 switches per string, and more parallel switches depending on the system size.

The controller also should be taken into account, the controller consists of micro-chip that cost in average $5. (i.e. Atmega 16 from ATMEL) and the other components used as accessories in the controller costs around $5. Another estimated extra expense is $90 (i.e. shipping, taxes, and soldering and wiring). The total cost of the controller unit should not exceed $100. If this controller is produced in large amount, the estimated cost will decrease.

Table 2 shows estimation for the switches cost for PV system consists of 9 modules and configured for the three Adaptive systems. As can be seen, the Adaptive PV string configuration has the minimal cost while the Adaptive PV-Inverter has the highest cost.

Table 2: Switches cost estimation for different Adaptive Systems

	Adaptive PV String	Adaptive PV Inverter	Adaptive PV DC/DC
Number of switches	$30	$40	$49
cost	$150	$200	$245

5. *Results, Analysis, and Comparison for Traditional and Adaptive systems*

5.1. Introduction

This chapter analyzes the performance and the annual losses of the traditional PV system configuration (central, string, and micro inverters configurations) using a mathematical calculation method and also using the Solar Advisor Model (SAM) as a software simulation tool. These losses are used as a reference for claiming the conclusion of the benefits of the Adaptive PV systems. This chapter also discusses the performance of the Adaptive PV systems. Each system is tested and validated using simulation, practical experiments, or calculation approaches. For the Adaptive PV-central inverter configuration, the systems have been simulated in MATLAB and experimentally tested. The experiments were conducted using a small prototype consisting of 9 PV modules and DC/DC converter to validate the simulation results. Results show that the proposed system is able to increase output power of solar PV array in real-time under shaded conditions by an average of 13% in simulation and by an average of 5% in practical experiments. For the Adaptive PV-inverter topology, the systems have been simulated in SAM and losses were calculated mathematically in similar way that the traditional systems were calculated. Results show that the proposed system is able to avoid up to 4% of the annual losses in the systems under low insolation conditions. Finally, For the Adaptive PV-String inverter configuration, the systems have been also simulated in

MATLAB and experimentally tested. The experiments were conducted using a real PV system consisting of 10 PV modules installed in Petroleum Institute in UAE to validate the simulation results. Results show that the proposed system is able to minimize the mismatching losses of solar PV array in real-time under shaded conditions to an average of 100% in simulation and to an average of 84% in practical experiments.

5.2. Traditional PV Configurations Analysis

5.2.1. Inverter Performance Characteristics

The efficiency of the grid connected inverter depends significantly on the ratio of the DC generated power to the nominal power of the inverter as shown in Figure 33. The performance of inverters is determined by the EURO efficiency η_{EU} or California efficiency η_{Cal} (26), (27). For example in the morning, when low radiation occurs across PV modules, the total generated power of each string decreases to a value that forces the string inverter to operate at a low efficiency point that leads to extra losses in the system. Another important value for the inverter is the optimum input DC voltage level that should also be taken into account in order to achieve the highest weighted efficiency. For example, for the same inverter, the efficiency will vary by changing the input voltage according to the inverter characteristics (28), (29). There is no general rule about the dependency of inverter conversion efficiency on DC input voltage. There are inverters that have their maximum efficiency at low voltages but there are also inverters that have their top efficiencies at high voltages and also inverters that have their maximum efficiencies at a medium DC.

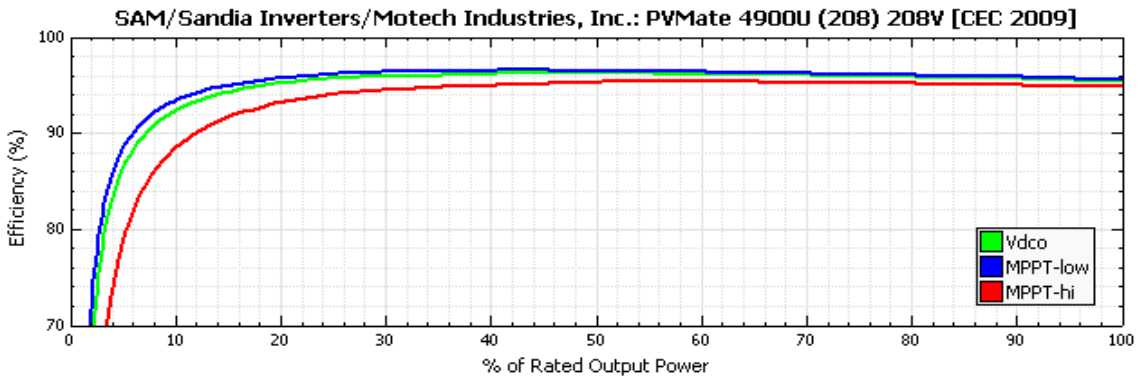

Figure 33: Central-Inverter's Efficiency-Power ratio Curve (30)

5.2.2. Analysis of traditional PV Systems

5.2.2.1. The Mathematical Calculation

The losses in the inverter due to variation in the input power during the day are known as Weighted Efficiency, as systems are installed in a wide range of solar resource regimes. For instance, if the inverter is oversized and the solar resource is marginal, the Weighted Efficiency would be a better predictor of system performance. Weighted Efficiency is calculated using the data taken at various levels of power according to the equation:

$$\eta_{wtd} = \eta_5 . F_1 + \eta_{10} . F_2 + \eta_{20} . F_3 + \eta_{30} . F_4 + \eta_{50} . F_5 + \eta_{75} . F_6 + \eta_{100} . F_7 \quad (14)$$

Where:

η_5, η_{10}, η_{20}, η_{30}, η_{50}, η_{75}, and η_{100}. - measured efficiency values at 5%, 10%, 20%, 30%, 50%, 75%, and 100% of rated power.

F_1, F_2, F_3, F_4, F_5, F_6, and F_7 - the weighting factors defined in **Table 3**.

Table 3: The Inverter Weighting factors [(26), Table 5-5]

Factor Inverter Power Weighting Factor				
Factor	Power level	High-Insolation[1]	Low-Insolation[2]	Effic. Values
F1	5%	0	0.03	0.85
F2	10%	0.04	0.06	0.93
F3	20%	0.05	0.13	0.957
F4	30%	0.12	0.1	0.96
F5	50%	0.21	0.48	0.962
F6	75%	0.53	0	0.96
F7	100%	0.05	0.2	0.957

1 – Based on irradiance and temperature data of Southwest US.

2 – Also known as European Efficiency.

5.2.2.2. The Analysis Tools

Solar Advisory Model (SAM) was used to verify the result of the proposed system. SAM allows the user to design the system by choosing the location of the system, components of the system such as PV module and inverter types, number of these components in the system and the configuration, tilt angled of modules, and financial method. The outputs of the simulated system are the annual energy of the system, the cost of system including the incentive and cash calculation. The annual energy can be generated using SAM(30) for different geographical locations such as Omaha, NE, Los Angeles, CA, Phoenix, AZ, Miami, FL, Seattle, WA, and Boston, MA. Different geographical locations are chosen based on the U.S. Photovoltaic Solar radiation map. Each city represents different

radiation zones in USA. In order to explain the advantage of the proposed system, a 4 kW grid connected PV system was analyzed. Configurations considered for analysis were the central PV system, strings system, and micro PV system. A three string system with 8 modules in series in each string chosen. The selected components are: Schott Solar 170Wp modules, Kaco new energy Gmbh : Bule planet 1502xi 240 V is taken as string inverter, Motech industries Icn. PVmate 4900U 208 V as central inverter and Enphase Energy M175-24-240-S 240 V as micro inverter. The efficiency of each configuration is developed and compared. The probability distribution functions (PDF) of the inverter's efficiency and the deviations of the efficiency values from the nominal efficiency value are studied. The comparison results are shown in Table 4. PDF curve of the string inverter in Seattle, WA, is also shown in Figure 34. The efficiency values are shown in the X-axis while the probabilities are in the Y-axis. Both can be seen in Figure 34. The highest column explains the nominal value of the inverter's efficiency. The other columns illustrate how frequent the efficiencies that do not meet the nominal value occur during one year. For example, the summation of the losses in Seattle is close to 4% yearly as shown in Table 4. In other words, the closer the values to the nominal efficiency, the smaller the losses in the inverter and the better the performance of the inverter.

5.2.3. Efficiency Comparison of traditional PV System Configurations

In Table 4, a comparison study of the inverter efficiencies for the configurations cited in last section is developed. Reviewing the results, the same system installed in different geographical locations with different insolation and weather status can perform better in placed where insloation is more stable.

Table 4: Comparison between Inverter Efficiencies for PV Configurations

	Losses in the Efficiency of the Inverters %		
Geographical Locations	Central-Inverter	String-Inverter	Micro-Inverter
Omaha	2.8%	2.9%	3%
LA	2.3%	2.4%	2.4%
Phoenix	2.5%	2.9%	2.9%
Miami	2.3%	2.5%	2.5%
Seattle	3.5%	3.7%	3.8%
Boston	2.9%	3%	3%

For example, in Phoenix, AZ, the system has yearly 3% losses in the inverter because of the efficiency responding characteristics, but in Seattle, WA, the system has approximately 4% losses because the radiation level varies. In other words, the annual low insolation portion in Seattle is larger than that in Phoenix. In order to illustrate the idea of losses in the inverter, an approximate study for inverter's efficiency PDF curves are taken for the high sample of efficiency value in Figure 34. For example, Phoenix, AZ, has a good response because the radiation profile gives the inverter the ability to work at

the optimal efficiency but the high temperature issue should be taken into account to reach a perfect case. Another example is Seattle, WA, in this case, because of the solar radiation profile, different operating points of the inverter efficiency will occur and the total losses of will be more as shown in Table 4.

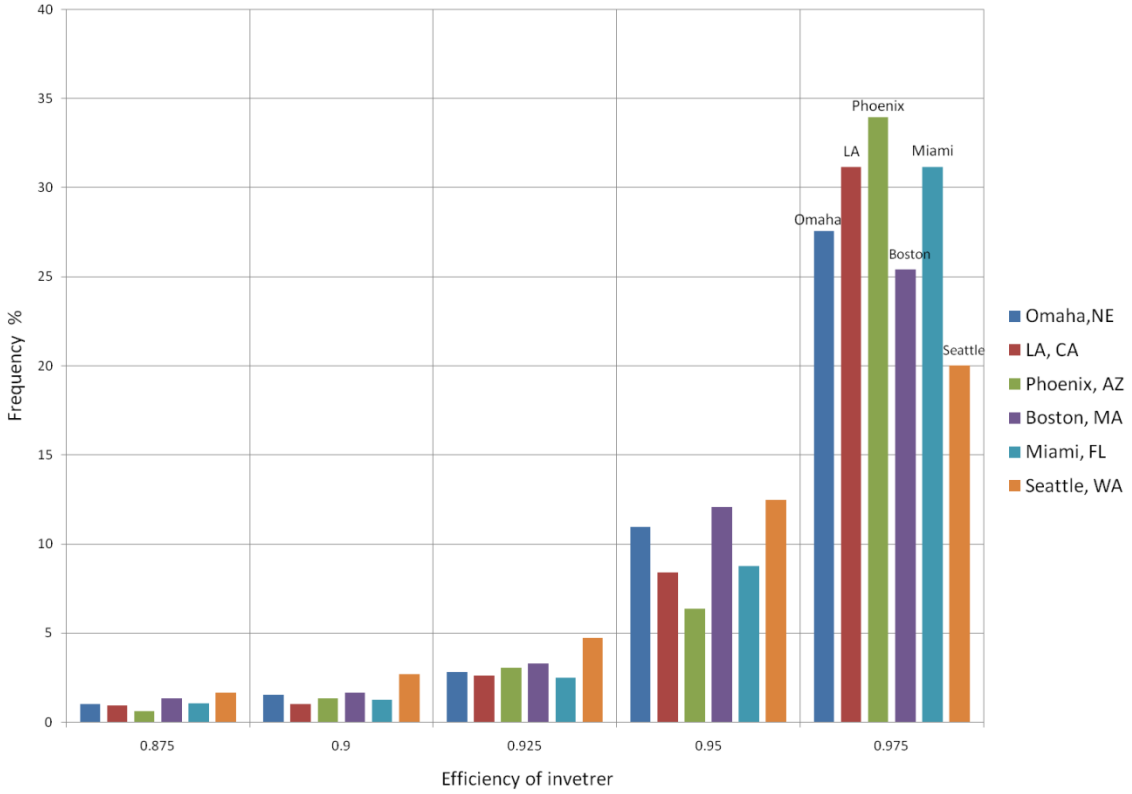

Figure 34: PDF Efficiency Curves of string Inverters for different locations

5.3. Verification Methodology for the Proposed Topologies

The proposed method will be compared to the traditional method using a simulation and prototype system. The adaptive PV topologies are simulated in MATLAB environment

using the simulation model discussed previously in chapter 2. All desired configurations of the system can be determined by the user. In order to compare the adaptive topologies to the traditional PV systems, practical experiments are conducted using prototype and real PV system. Results are compared as shown in Figure 35.

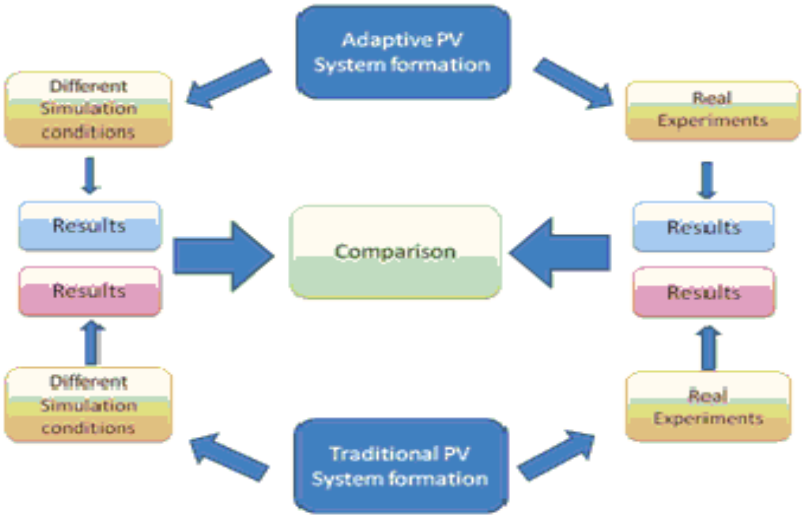

Figure 35: Verification methodology for PV Systems

5.4. Adaptive PV central-inverter configuration results and analysis

5.4.1. Simulation Result for Adaptive PV central-inverter configuration

The nine module array system shown in Figure 22 is used to explain the proposed adaptive PV system. The model will be used to generate preliminary results for comparison between the proposed adaptive system and the traditional fixed PV system under the normal operation condition of insolation. In this comparison, the fixed system is the central inverter system. During normal operational conditions, the simulation curves of the fixed and adaptive PV systems are identical because of the similarity of the modules' configuration. In full-shading conditions (the case of dissimilar irradiance

across the PV field that occurs because of moving thick clouds, trees, or any adjacent structure that makes a full shadow), cases of one, two, …, eight shaded PV modules have been simulated and compared for both systems. Figure 36 shows the comparison results for two and three shaded modules. Power is scalable in simulation model and the magnitude can be changed according to the required power level of PV system. Table 5 provides a summary of the results of all simulation cases.

In Figure 36 (a), the case of two shaded modules is analyzed. The fixed system has two shaded modules from different strings that activate the bypass diodes and generate multiple peaks while the adaptive system rearranges the modules in MPV and SPV strings to get better performance, thus improving the efficiency of the system. As can be seen in Figure 36 (a),, the adaptive system has a single peak that has a value higher than the fixed system even though the fixed system has two peaks. However, both of them have a lower value than the peak of the adaptive system. In this condition the efficiency improvement $\eta = (MPP_{fixed}/MPP_{adaptive})$ is 13%, without taking into account the DC/DC efficiency that should be applied to one module.

In Figure 36 (b), the case of three shaded modules is analyzed. Each string has one shaded module. While the total number of shaded modules matches the number of strings, the adaptive system rearranges the modules to achieve the desired configuration. Both the fixed and adaptive systems have the same peak value. That means that while both systems act alike, the adaptive system has an advantage in that its voltage output matches the inverter nominal voltage while the fixed does not. In this case, the DC/DC converter will not be used and as a result no additional losses are incurred.

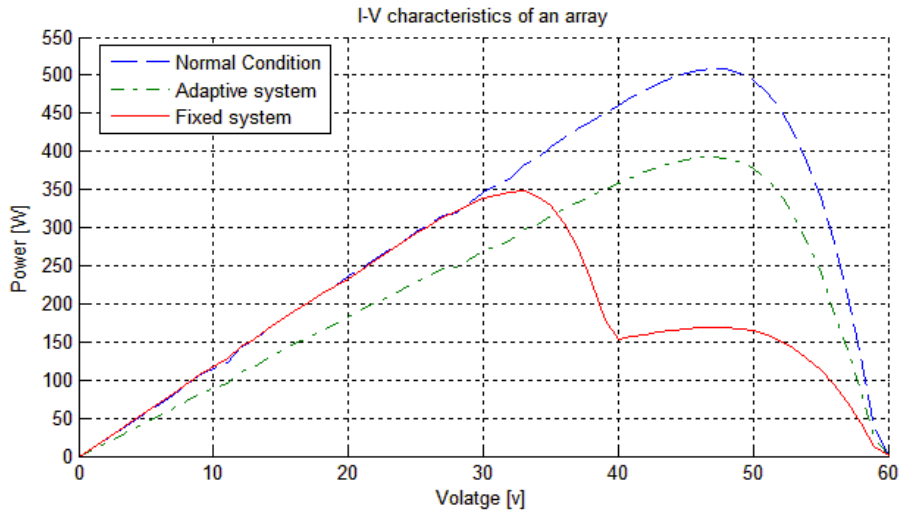

(a) Simulation results for Two Shaded modules

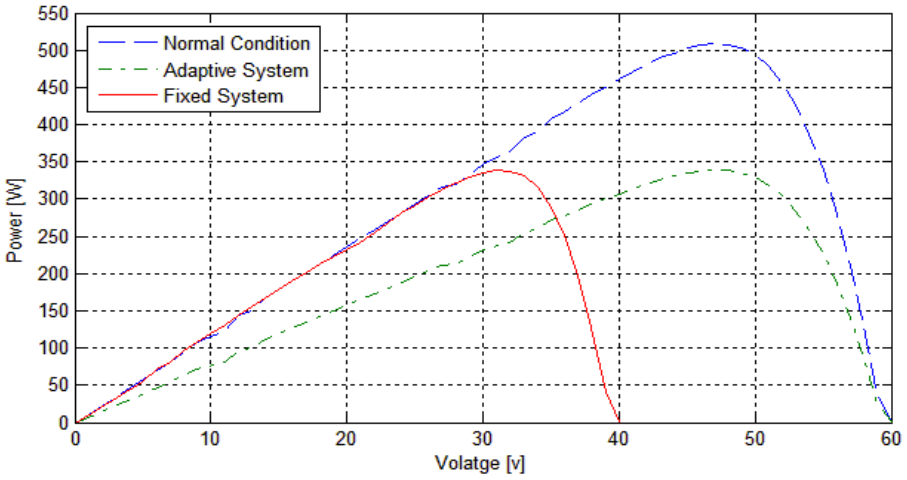

(b) Simulation results for Three Shaded modules

Figure 36: Simulation results for Two (the top) and Three (bottom) Shaded module (25)

5.4.1.1. Efficiency Comparison between Adaptive PV Central-Inverter and Traditional Central-Inverter PV Configurations

The efficiency results are shown in Table 5. The traditional fixed PV system has more cases of shading because of the fixed connections between the modules. However, in order to compare both systems, the same shading cases across the PV modules are considered. The comparison doesn't include the actual efficiency of the DC/DC

converter. The simulation assumes that an ideal DC/DC converter is utilized with no losses. The actual DC/DC efficiency will be included in the next section. The best performance occurs when five modules are shaded (a fully-shaded string and two modules from another string).

Table 5: Comparison between Fixed and Adaptive PV System for Different Shading Conditions (25)

Configuration		Connected to	η improvement = Padv/Pfx	Number of shadowed modules
1	One module connected to DC/DC +	Two strings	13%	2
2		One string	31%	5
3	Two modules connected to DC/DC +	Two strings	22	1
4		One string	18%	4
5	One or Two module/s connected to DC/DC	Alone	0%	7
6	One, Two, or T ree strings	Alone	0%	8, 6, or 3

As can be seen in Table 5, approximately 30% of the lost energy in the fixed configuration can be generated using the proposed adaptive system. This is because of the string voltage matching technique used in the proposed system. The worst performance occurs when one or two modules are active and all other modules are shaded (disconnected). In this case, the DC/DC converter will ideally step up the voltage of the module(s) to match the inverter's required input voltage. The results in Table 5 also show that the overall efficiency of the proposed adaptive system is much higher than the efficiency of the traditional fixed system for other cases that may occur more frequently.

5.4.2. Prototype system design and development

5.4.2.1. The Prototype Set

Figure 37 (a) shows the solar PV module test platform. A prototype is built using 9-PV modules in order to validate the proposed system and efficiency results obtained via the simulation. The prototype consists of Nine PV modules, each rated at 1-Watt and 6-Volts at MPP. The I-V curves of the formed strings of the prototype are illustrated in Figure 37 (c). As can be seen, the characteristics of all strings are almost identical and this support the comparison results in the following experiments; a 3-Amps and 55-volts DC/DC converter with adjustable output voltage level in range of 5 to 55 volts is also chosen; bypass diodes for each module; variable resistive loads; and miscellaneous conductors and connecters for connection among the modules DC/DC. Table 6 shows the experimental result conducted in Omaha, NE, USA during the first week of November 2010. The experiments were executed in sunny and clear sky conditions. The actual experiments were performed to mirror the simulation case studies (One, Two, Three, Four…, Eight, shaded modules). Multi-meters were used to measure the DC voltage and current of the strings and modules before and after implementation of the DC/DC converter.

Table 6: Comparison between Simulation and Practical Results of Adaptive PV central-inverter System for Different Shading Conditions

	Available configuration		method	η = Padv/Pfx
3	Two modules connected to Dc/Dc with….	One shaded module	simulation	22%
			real	5%
1	One module connected to Dc/Dc with….	Two shaded modules from different strings	simulation	3%
			real	0%
2		Five shaded modules	simulation	31%
			real	11%

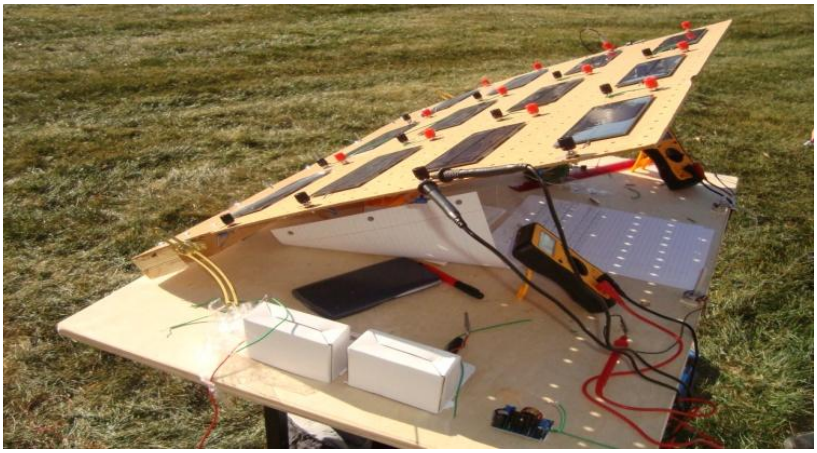

(a) The prototype setup

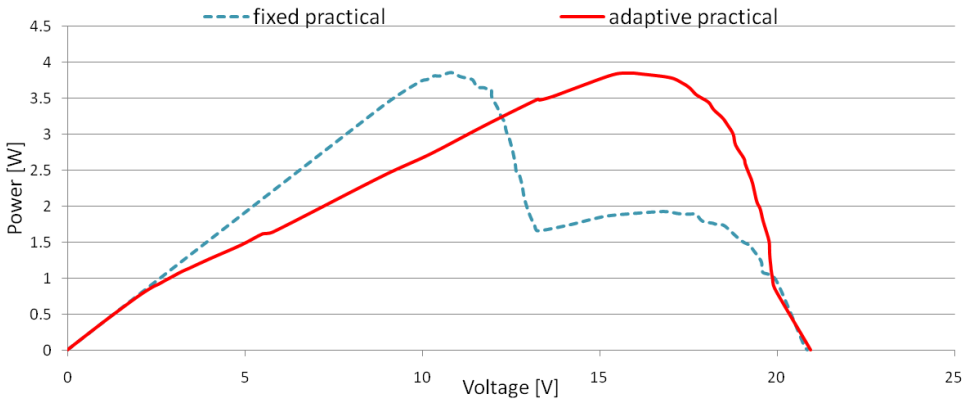

(b) Prototype Result for Two Shaded Modules

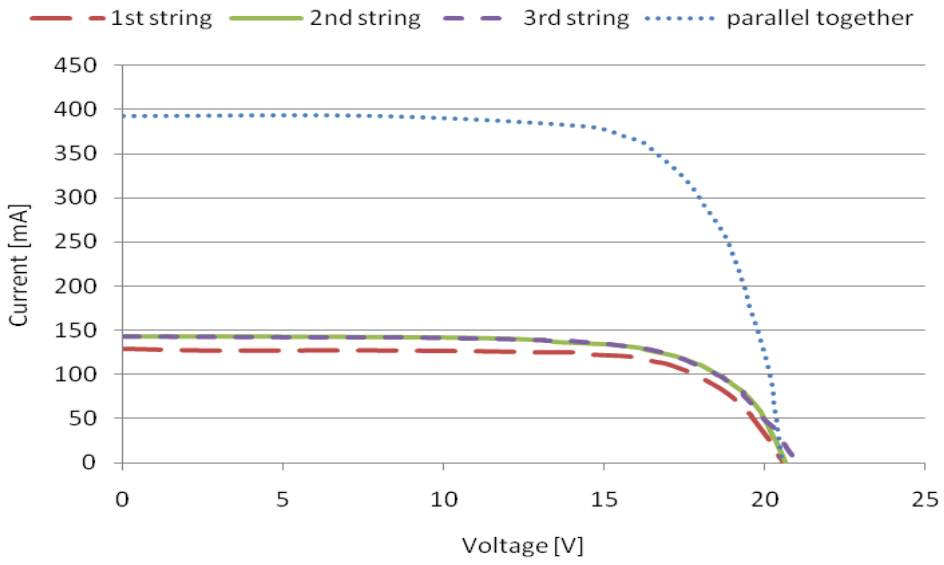

(c) I-V curves (bottom) for the strings of the prototype

Figure 37: Adaptive PV Central-Inverter Configuration Prototype and Result for Two Shaded Modules and I-V curves for the strings of the prototype

5.4.3. Results & Analysis

Figure 37 (b) shows the experimental results of the prototype system for two-shaded modules for the fixed configuration and proposed adaptive system. The curves are determined point by point using an adjustable resistance as PV generator load. As can be seen in the Figure, the actual behavior of the actual systems and simulated systems are very similar. The multiple peaks shown are for the fixed system due to the bypass diode. As can be seen in Figure 38, the practical results approximately match the generated results of the simulation model. The simulation results are scaled to match the Prototype results. The power axis is multiplied by 10 for clearer result. Table 6 shows a comparative study of the overall efficiency between the simulation and the prototype results for different operational cases. The comparison includes the actual efficiency of the DC/DC converter obtained from the manufacturer/published or common data.

As discussed in the simulation section, the best performance occurs when five modules are shaded. In this case, the DC/DC converter does not affect the system by reducing its overall efficiency. The reason for this is that the DC/DC is only responsible for one module while the other modules work normally. The worst case occurs when one or two modules are active and the other modules are shaded (disconnected). In this case, the overall efficiency of the system will decrease as the actual DC/DC efficiency is included. Even though the efficiency of the adaptive system may decrease according to the configuration, the results in Table 6 show that the efficiency of the proposed adaptive system is higher than the efficiency of fixed system. Although the prototype results for the output power curves match the curves generated using the simulation results, a reduction in the output power in the prototype curves is present.

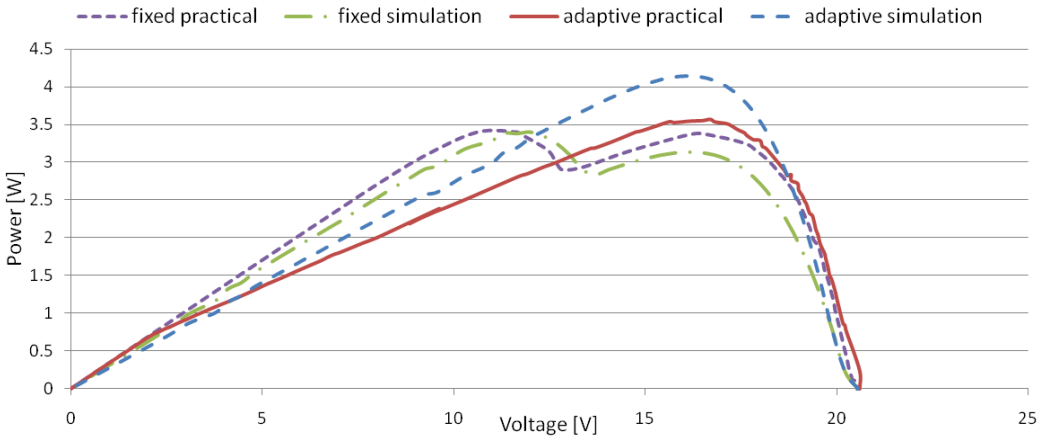

(a) One shaded module

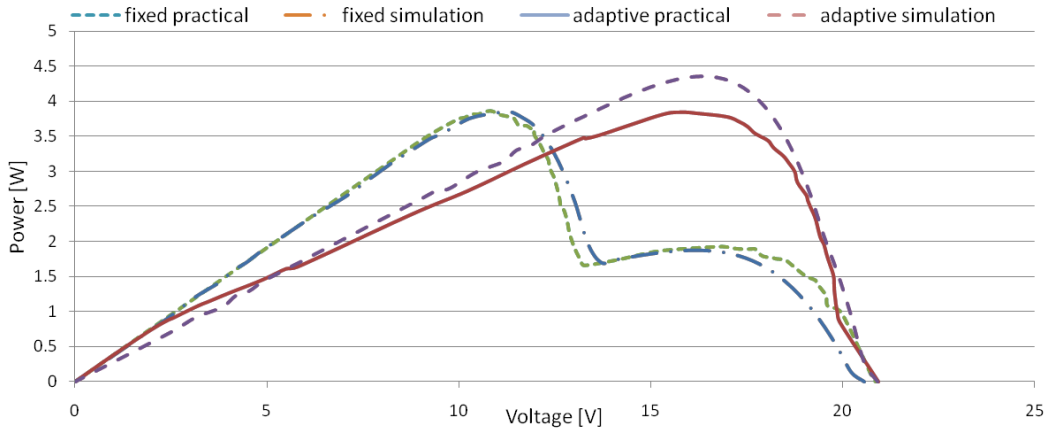

(b) Two shaded modules

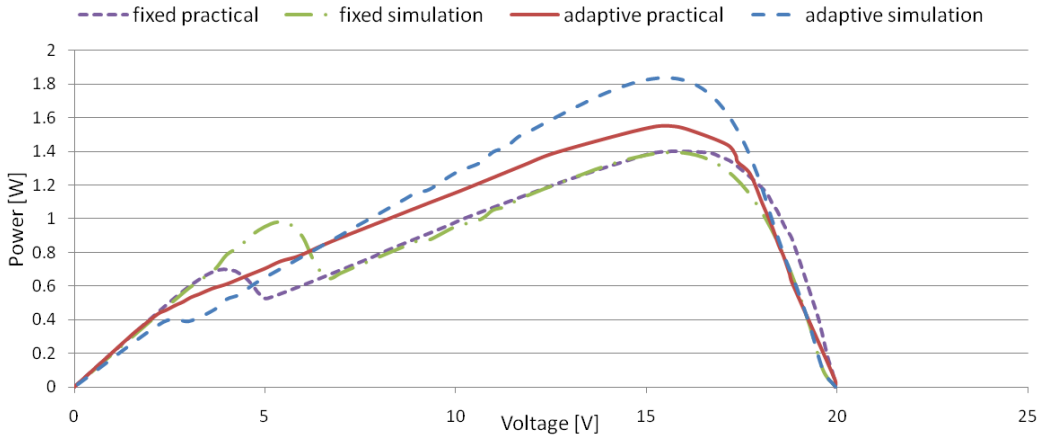

(c) Five shaded modules

Figure 38: Simulation and practical results for one, two, and five shaded modules

This may be due to the efficiency of the real DC/DC converter which varies between 80-85% ± 5% or the power rating size of the DC/DC converter as shown in Figure 39 (a). Figure 39 (b) illustrates the efficiency improvement comparisons between the simulation and prototype results for both systems during different shading conditions using a DC/DC converter. The simulation and prototype results validate the proposed adaptive system.

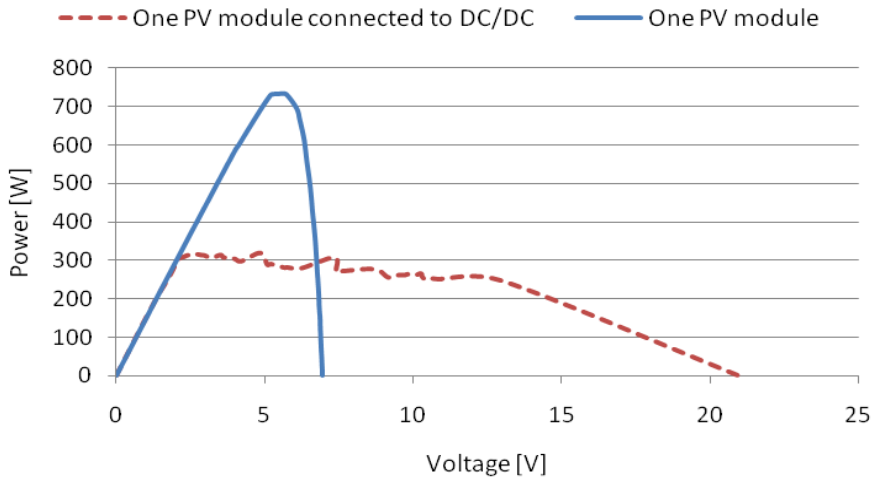

(a) DC/DC response for one module

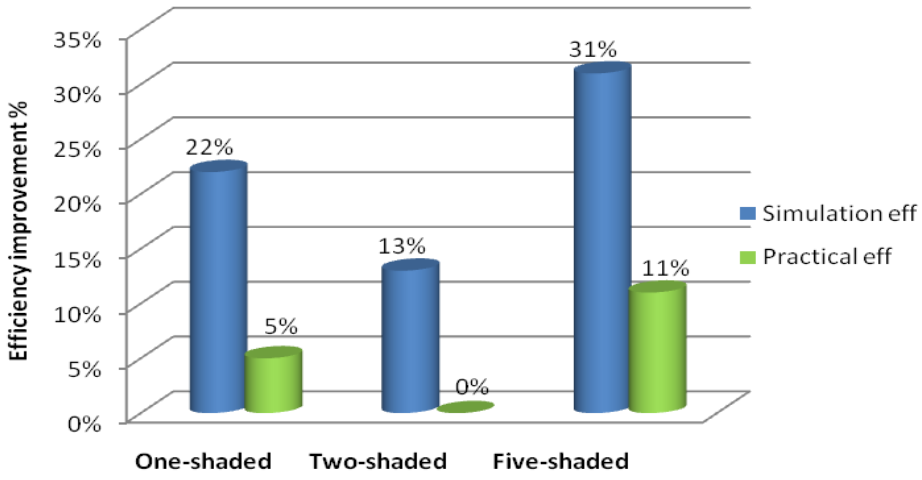

(b) Efficiency improvement comparison

Figure 39: Adaptive PV central-inverter efficiency improvement comparison between simulation and practical results for Different Shading Conditions and DC/DC response for one module

5.5. Adaptive PV-Inverter Topology Results and analysis

5.5.1. Advantages of Inverter Based Adaptive System

PV system undesired effects are tackled in this topology, the Shading Effect, the Mismatching Effects, and a low radiation losses in the inverter depends on the configuration.

In the adaptive system concept, which offers flexible connections between modules, the shaded module can be eliminated by disconnecting it from the array. The process can be achieved by the switching matrix and the control algorithm that selects the optimum configuration after removing the shaded modules.

Another advantage of adaptive system is also to avoid the multiple peaks phenomenon in power curve that occurs because of bypass diodes in traditional PV system (Fixed system). In this case a simple MPPT can be used instead of the complex one. Improvement in the adaptive system curve is seen. There are no longer local peaks and the system works as normal operating condition. The efficiency of the grid connected inverter depends significantly on the ratio of the DC generated power to the nominal power of the inverter as shown in Figure 33.

The concept of adaptive PV system allows us to rearrange the modules in different configuration and connect them to different inverters to match its maximum efficiency.

As also discussed in section 5.2.1 pp 71, the losses in the inverter due to variation in the input power during the day are known as Weighted Efficiency has losses according to the radiation level. **Table 3**, Table 4 and Figure 34 illustrate these losses.

In Adaptive PV-Inverter system, equation (9) will be modified in which the losses in the inverter due to different efficiency values can be eliminated. The new equation may have single factor to affect the overall efficiency. In other words, the annual low insolation portion in Seattle is larger than that in Phoenix. This conclusion gives the adaptive system more potential to be applied in such locations with unstable insolation areas as shown in Figure 34. As can be seen, there is 4% annual losses in Seattle that can be recovered using the adaptive-inverter topology. The losses are minimized because the system will operate at the inverter's optimal operating point by rearranging the PV modules in suitable configurations. The calculation proves the improvement and SAM simulation curve of the inverter shows a potential for efficiency improvement.

5.6. Adaptive PV Central-Inverter Configuration Results and Analysis

5.6.1. Simulation And Practical Results

A MATLAB simulation model and an actual test were conducted using two strings of three series connected PV modules, 50 W each, to verify the proposed topology. Shading over one, two, and three PV modules from different strings was examined using the traditional system and the proposed configuration. Figure 40 shows the results of the simulation and practical experiments. As can be seen in Figure 40 (b), the traditional system response for shading is represented by generating multiple peaks in P-V curve. These peaks represent the losses in the system.

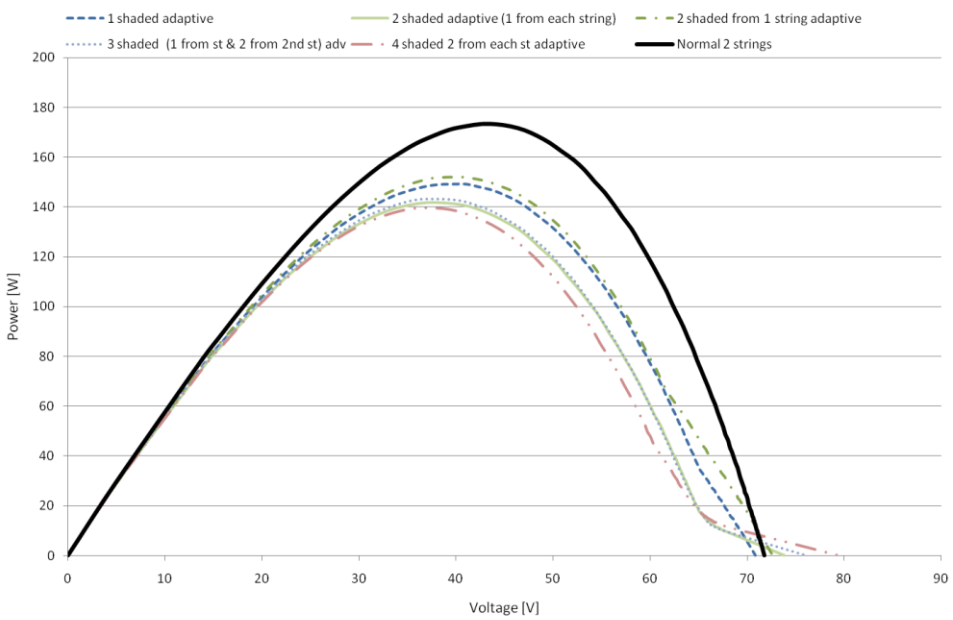

(a) Adaptive system P-V curves

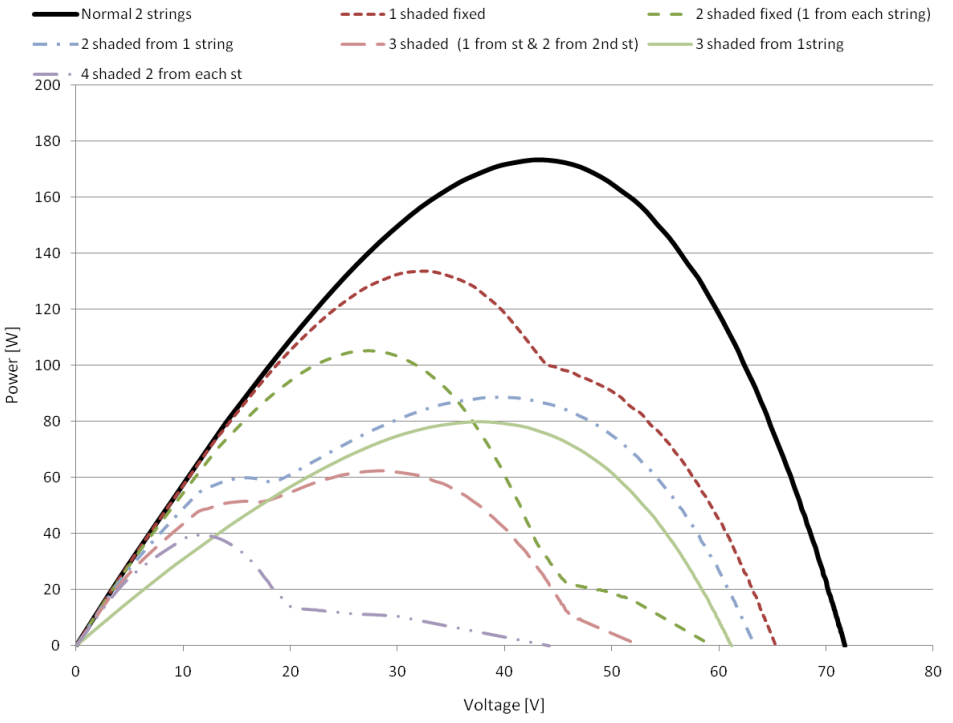

(b) Traditional System P-V curves

Figure 40: Fixed and adaptive system results for different kinds of shading patterns

These results in Figure 40 (b) shows that the proposed system smoothes the P-V curve shape to have single peak in the curve. P-V curve no longer has multiple peaks, thus, minimizing the shading losses in the system. Figure 41 (a) shows the I-V tracker model number PVPM 1000 which was used to measure the electrical characteristics of the PV system and transfer the measured data to Excel file. Figure 41 (b) shows the actual PV system in Petroleum institute, UAE. The measurements were taken in February 23rd and 24th, 2011. For more information about the electrical specification of the PV system used in this section, see Appendix C.

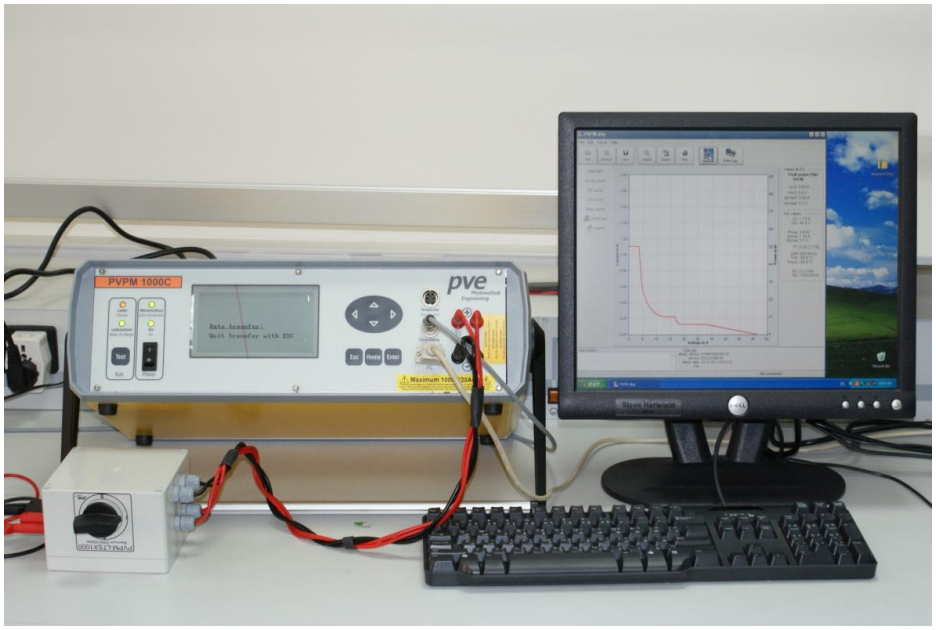

(a) I-V Tracker Model Number PVPM 1000

(b) PV System in Petroleum Institute, UAE

Figure 41: I-V tracker and an actual PV system in Petroleum institute, UAE

5.6.2. Results & Analysis

Two shaded modules from the same string is taken as sample to discuss and compare the P-V curves of the practical experiments. As can be seen in Figure 42, the normal operation condition is illustrated by the highest peak in Figure 42 (a) and (b). Traditional system is represented by the multiple peaks curves with low peak value than other curves while the Adaptive system is denoted by the middle curve in Figure 42 (a) and the overlapping curve in Figure 42 (b) that occurs as a result of ideal simulation result. Ideally, when module is shaded and additional modules is added to the same string, the system will return to the normal operation as shown in Figure 42 (b) and P-V characteristics will overlap the normal condition while practical response is a little different due to the bypass diode losses and inner resistant of the shaded PV module. As can be seen, adaptive and no-shading (normal) P-V curves are not identical. Figure 42 (b) illustrates the difference. The most important observation is that both simulation and practical result represent one single peak in the P-V curve, which is the main concern to the PCUs. As discussed in the previous proposed topologies, single peak means more efficient system and fewer losses (mismatching losses).

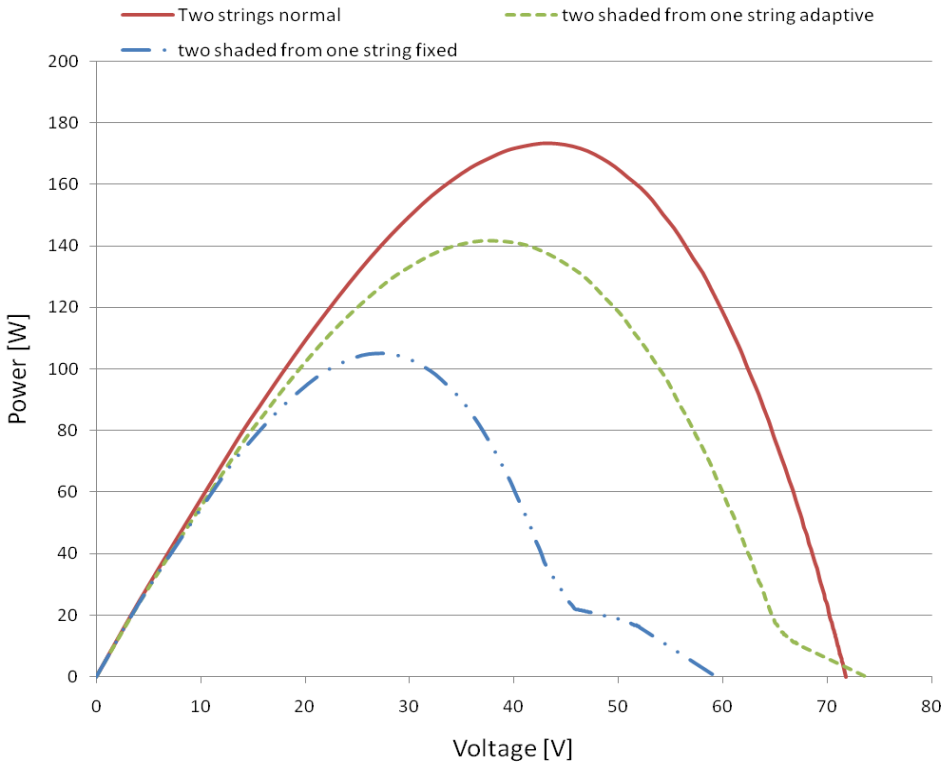

(a) Practical results for two shaded modules for Adaptive and Traditional systems

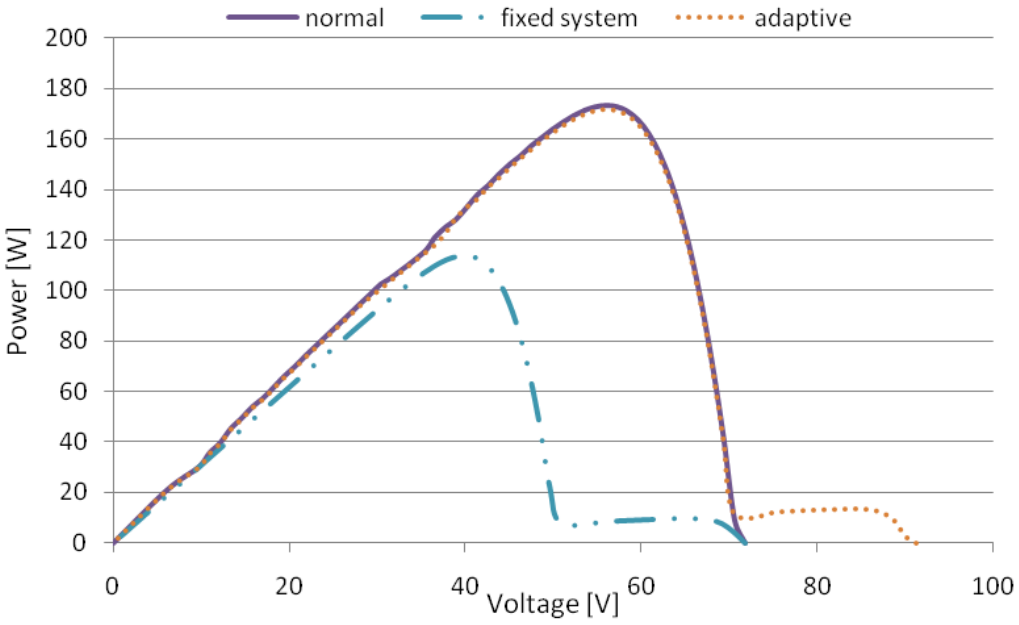

(b) Simulation results for two shaded modules for Adaptive and Traditional systems

Figure 42: Practical and Simulation Results For Two Shaded Modules

Table 7 shows a comparison of the maximum power value for both traditional and adaptive PV string-inverter configuration practical results according to the shading pattern. The table also shows the losses due to shading effect for both systems. In the traditional system, the losses increase as number of modules in the system increases as shown in Figure 43. In the adaptive system, the losses value decreased to an average of 16%. In other words, results show that the proposed system is able to minimize the mismatching losses of solar PV array in real-time under shaded conditions to an average of 100% in simulation and to an average of 84% in practical experiments.

This improvement in the losses is due to the additional PV modules that compensate the power and voltage drop in the shaded string. Another important observation in losses values of Table 7 is that no matter what shading pattern affected the system, the losses of Adaptive PV string-inverter configuration are almost constant and this is a very promising result for large PV installation.

Table 7: Comparison Results for Shading Losses in Adaptive PV string-inverter configuration and Traditional Systems

	Pmax Normal (no shading) =		173.31 [W]	
number of shaded modules	Pmax [W] Traditional	Pmax [W] Adaptive	losses in Traditional	losses in Adaptive
One	133.50	149.30	23%	14%
Two from same string	88.50	152.16	49%	12%
Two from different strings	105.12	141.74	39%	18%
Three from different strings	62.31	143.35	64%	17%
Four (two from each string)	39.50	139.76	77%	19%

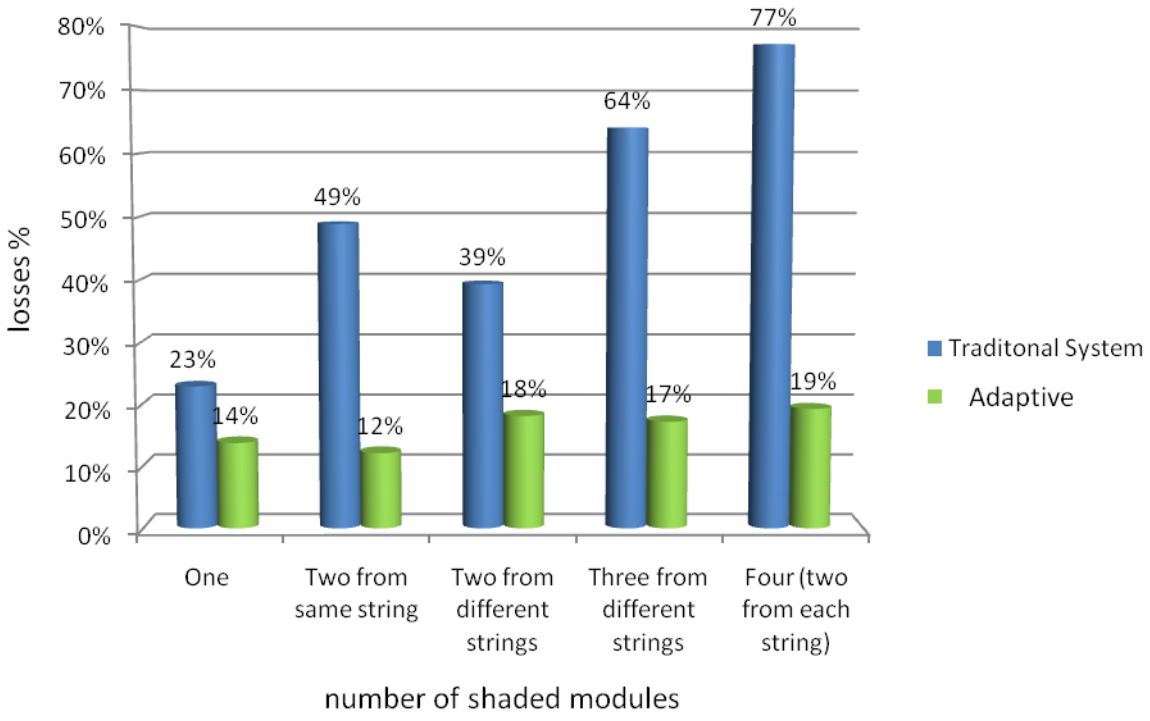

Figure 43: Losses Comparison Between Adaptive PV string-inverter configuration and Traditional Systems

6. *Summary and Future Work*

6.1. Summary

This thesis proposed new methods to adaptively overcome the electrical mismatching losses in existing PV configurations, especially due to shading and low radiation where power generated from these systems decreases. The thesis also investigated the technical aspects of different proposed strategies. The proposed systems have been validated under shading effects using a simulation and prototype experiments. The results of this study indicate that the proposed systems improve the efficiency under differing operational conditions by tracking the optimal configuration of the components. A comparison between the traditional PV system and the proposed adaptive systems are given. Three topologies were proposed, adaptive PV central-inverter configuration, adaptive PV-inverter topology, and Adaptive PV string-inverter configuration.

In the first proposed topology, the adaptive PV central-inverter configuration is based on the flexible switching matrix (FSM) to reconfigure the connections between PV modules and power conditioning components. Preliminary results show that an average of 13% of the lost energy during shading can be recovered using this system.

The second proposed topology, the adaptive PV-Inverter system is proposed for some applications in terms of annual energy losses, such as low radiation conditions, to minimize the losses in the inverter of the PV system. The analysis results with SAM verify the behavior of traditional PV configurations and compare them together. Calculation of the adaptive system is done to verify the performance improvement. New switching matrix architecture is proposed to achieve adaptive connection between PV

modules, preliminary results of adaptive PV-Inverter system show that an average of 4% of the annual lost energy due to the inverter efficiency characteristics during low radiation conditions can be conserved using this topology. But it required huge number of switches to achieve different configurations.

A revised version that combines the advantages of the first and second proposed topology is called the Adaptive PV string-inverter configuration based on an advanced flexible switching matrix (FSM). This last is proposed as a feasible solution for the PV system to reconfigure the connections between PV modules and power conditioning components such as the inverter using less number of switches. Adaptive PV string-inverter configuration is very suitable for upgrading the existing traditional PV systems to a smart, efficient, and adaptive PV system. Preliminary results show that the lost energy due to electrical mismatching losses between the PV strings can be recovered using this system. Results show that the proposed system is able to minimize the mismatching losses of solar PV array in real-time under shaded conditions to an average of 100% in simulation and to an average of 84% in practical experiments.

Finally, a statistical analysis for choosing the feasible and efficient configuration according to the size of the system was discussed. The results show that for small applications up to 10 kW, Adaptive PV central-inverter configuration using DC/DC converter is feasible while Adaptive PV string-inverter configuration, which uses large number of parallel strings, is applicable for large scale PV installations. As also a result, the adaptive PV-Inverter topology is not feasible and can be replaced by the Adaptive PV string-inverter configuration.

6.2. Future work

After the work in adaptive system, more energy can be generated from PV system. This idea paves the way for future research where more energy can be stored in case of PV system using storage devices (battery). The future work can look into the mismatching losses during charging process and then propose a new flexible Photovoltaic/Battery charging System (PVBS), where the interconnection of the system is dynamically changing based on current shading conditions across PV modules to provide intelligent system, as well as to provide flexibility, performance, and efficiency enhancement for the PV system. PVBS is expected to: 1) provide a battery charging efficiency improvement over existing employed topologies, and 2) provide new means to match the computing load with the PV system performance metrics shading and mismatches. Figure 44 shows the possible layout of the adaptive PV/Battery system using two kinds of Batteries (micro and string battery).

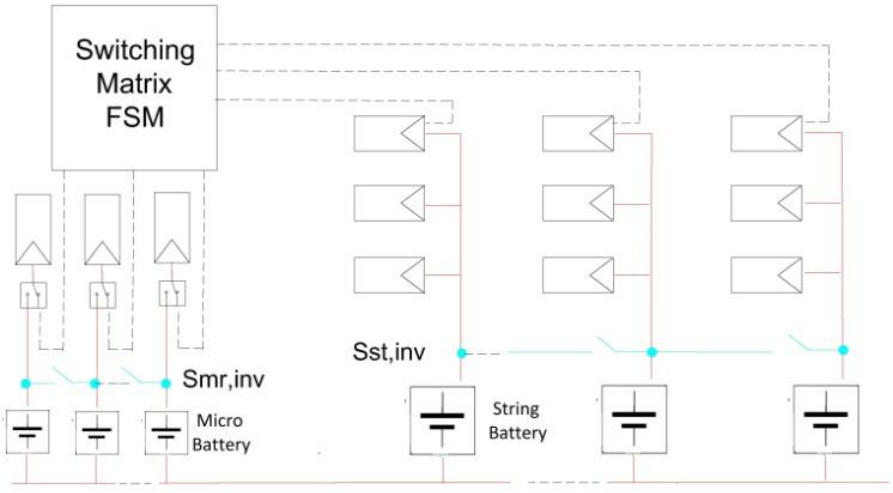

Figure 44: Imaginary layout of future research using battery bank

Appendix A

A.1 Measurement of Solar Radiation on Earth's Surface

The global horizontal irradiance is usually measure by Weather stations. The solar radiation are measured by special instruments such as, *pyrheliometer* that measures the direct component of solar radiation at normal incidence. The instrument should always be aimed directly at the Sun, *pyranometer* that measures the total radiation, and Sunshine recorders that are used to indicate the amount of sunshine at a given location. To measure the diffuse irradiance, a shading ball or ring can be used to permanently shade the Pyranometer. Figure 45 shows pictures of the three devices used to measure different irradiance components (4) (6).

Figure 45: Pyranometer (left top), Two-axis tracked pyrheliometer (left bottom), Pyranometer with shading ball (right) (5)

A.2 The global irradiance density

As can be seen in Figure 46, the total specific radiant power, or radiant flux, per area that reaches a receiver surface is called irradiance. Irradiance is measured in W/m². When integrating the irradiance over a certain time period it becomes solar irradiation. Irradiation is measured in either J/m² or Wh/m². For daylighting purposes, only the visible part of the sunlight is considered. The analogous quantity to irradiance for visible light is the illuminance. This uses the unit lm/m² (lumen/m²) or lx (lux).

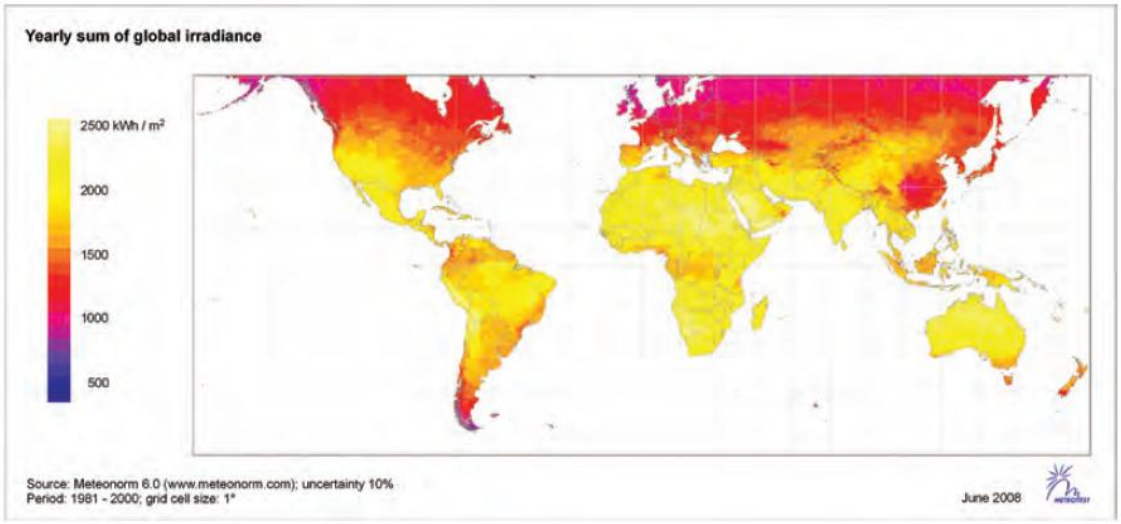

Figure 46: Total annual amount of solar energy per unit area for horizontal planes (1) **pp 146**

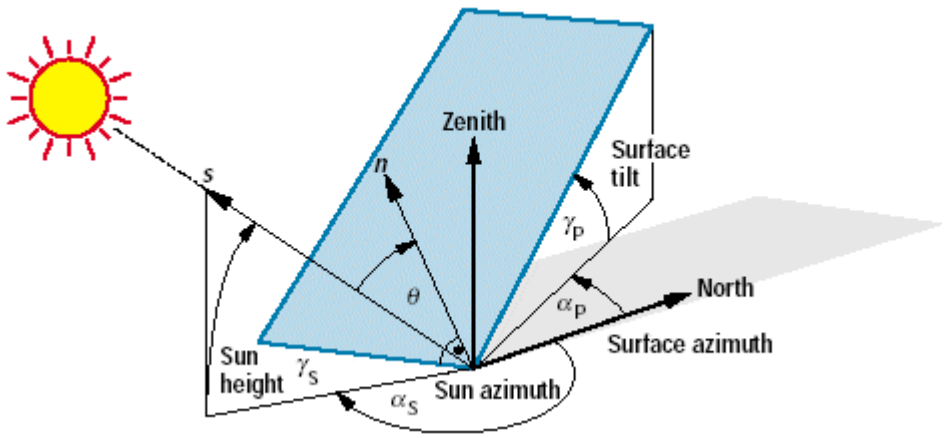

Figure 47: Angles to define the position of the sun and the orientation of a tilted plane (5)

A.3 The apparent motion of the sun

The apparent motion of the sun and its position is relative to a fixed observer at a point on the earth. The position of the sun depends on the time of year, the time of the day, and latitude as shown in Figure 48 . The earth travels in space on an elliptical orbit around the sun, with its axis tilted, which causes the seasonal variations in the sun's path across the sky. Simultaneously the earth makes 24-hour full circles around its axis, causing the sun to rise and set every day.

Two angles are used to define the position of the sun. *The solar altitude angle (sun height)* is the vertical angle between the sun ray and the horizon. This angle complements the Zenith angle while sum of both angles always = 90^0. *The solar azimuth angle* is the horizontal angle between a reference direction (the south in north atmosphere) and the sun. This angle varies from 180^o to 180^o as illustrated in Figure 47.

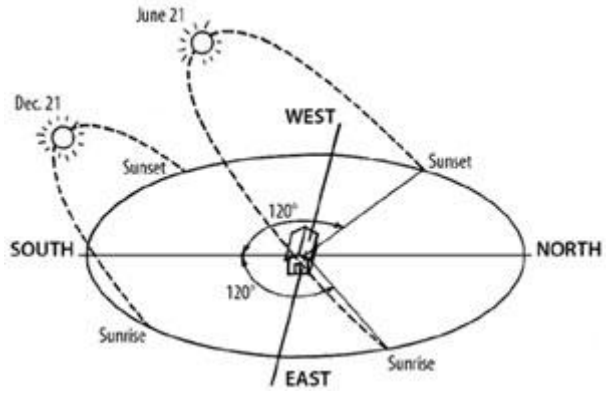

Figure 48: spherical solar daily motion for Jun and December

A.4 The sun path

Sun path diagrams are representations on a flat surface of the sun's path across the sky. They are used to easily and quickly determine the location of the sun at any time of the day and at any time of the year. Each latitude has its own sun path diagrams.

As can be seen in **Error! Reference source not found.**, the horizon is represented as the outer circle, with the observer is in its center. The concentric circles represent the angle of the sun altitude angle. The radial lines represent its angle relative to due south.

The paths of the sun on the 21st day of each month are the elliptical curves. For example, curve of (March) is the same as curve of (September). The vertical curves represent the time of day. Morning is on the right (east) side of the diagrams and afternoon on the left (west).

Example :

Omaha **Latitude**: (41°15'30.996"N)

Longitude: (95°56'15"W)

Time zone: UTC-6 hours

In order to maximize the energy production of the photovoltaic system, PV modules are usually tilted by an angle to maximizing the direct irradiance reaching the surface. The optimum tilt angle with respect to the horizontal surface of the earth can be calculated for each specific site; however, it is usually set within range of $\pm 15^{o}$ of the site latitude (6). Thus, the irradiance components received by the tilted surface of the PV array are different from those provided by the weather stations. Accordingly, different models must be used to estimate the different irradiance components on the surface of the PV modules from those provided by the weather stations which is beyond the discussion of this work.

Appendix B

B.1 Technology Trends of PV

According to IEA solar PV roadmap 2010, PV technology development sectors are divided into five main subsectors as follows:

Crystalline silicon (c-Si) modules represent 85-90% of the global annual market today. C-Si modules are subdivided in two main categories: Single crystalline (sc-Si) and Multi-crystalline (mc-Si).

Thin films currently account for 10% to 15% of global PV module sales. They are subdivided into three main families: Amorphous (a-Si) and Micromorph silicon (a-Si/μc-Si); Cadmium-Telluride (CdTe), and Copper-Indium-Diselenide (CIS) and Copper-Indium-Gallium-Diselenide (CIGS).

Emerging technologies encompass advanced thin films and organic cells. The latter are about to enter the market.

Concentrator technologies (CPV) use an optical concentrator system which focuses solar radiation onto a small high-efficiency cell. CPV technology is currently being tested in pilot applications.

Novel PV concepts aim at achieving ultra-high efficiency solar cells via advanced materials and photo-chemical processes. They are currently the subject of basic research.

Figure 49 shows the relationship between Current efficiency performance and price of different PV module technologies.

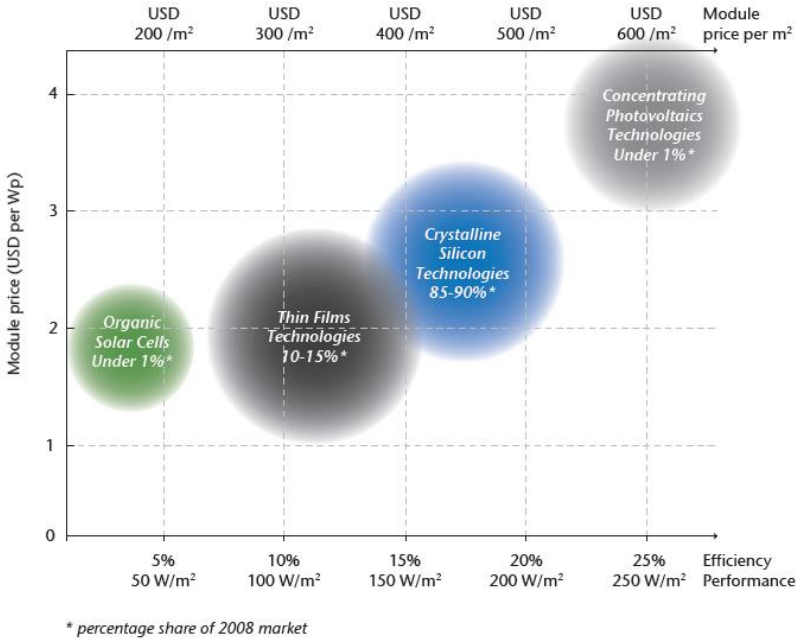

Figure 49: Current performance and price of different PV module technologies (3)

Table 8 shows the efficiencies of these technologies.

Table 8: Current efficiencies of different PV technology commercial modules (3)

Wafer-based c-Si		Thin films		
sc-Si	mc-Si	a-Si; a-Si/µc-Si	CdTe	CIS/CIGS
14-20%	13-15%	6-9%	9-11%	10-12%

Appendix C

C.1 PV system specifications

The PV system used in chapter 5 to conduct the experiments for the Adaptive PV String-Inverter Configuration has the following specifications:

Location: Roof top system, Petroleum Institute, UAE

Number of PV modules: an Array of 10 panels

Module's material: CIGS, thin-film

Tilt angle: 25˚ (north earth atmosphere)

Total power output: 500W

Provided by PTL Solar, Dubai, UAE

Parameter	**Rated Value**
Maximum Power (W)	50
Tolerance (%)	±10
Maximum power voltage	16.8
Maximum power current	3.0
Open Circuit voltage (Voc)	25.2
Short Cir uit current (Isc)	4.1
Max system voltage (Vdc)	600

References

1. Gaiddon B, Kaan H, Munro D. Photovoltaics in the urban environment : Lessons learnt from large-scale projects. London; Sterling, VA: Earthscan; 2009.

2. International energy outlook http://www.eia.doe.gov/oiaf/ieo/electricity.html [Internet].: Energy Information Administration; 2010.

3. Technology roadmap solar photovoltaic energy. [Internet]. Paris: OECD/IEA; 2010.

4. Tiwari GN, Dubey S. Fundamentals of photovoltaic modules and their applications. Cambridge: Royal Society of Chemistry; 2010.

5. Technology fundamentals http://www.volker-quaschning.de/articles/fundamentals1/index.php [Internet].: Renewable Energy World [updated 05/2003.

6. Dunlop JP, National Joint Apprenticeship and Training Committee for the Electrical Industry. Photovoltaic systems. Orland Park, Ill.: American Technical Publishers, Inc.; 2010.

7. Planning and installing photovoltaic systems a guide for installers, architects, and engineers. Sterling, VA: Earthscan; 2007.

8. Applied photovoltaics. London: Earthscan; 2007.

9. Tutorial http://zone.ni.com/devzone/cda/tut/p/id/7230 [Internet].: National Instruments (NI); Dec 4, 2009.

10. Saiju R. Hybrid power system modelling-simulation and energy management unit development [dissertation]. Kassel University; 2008.

11. Kheswa EFM, Davidson IE. In: Model of a photovoltaic fuel-cell generator. AFRICON, 2004. 7th AFRICON conference in africa; ; 2004. p. 735,739 Vol.2.

12. Patel H, Agarwal V. MATLAB-based modeling to study the effects of partial shading on PV array characteristics. Energy Conversion, IEEE Transactions on. 2008;23(1):302-10.

13. Rashid MH. Power electronics handbook. San Diego, CA: Academic Press; 2007.

14. Omran W, University of Waterloo. Dept. of Electrical and Computer Engineering. Performance analysis of grid-connected photovoltaic systems. Waterloo, Ont.: University of Waterloo; 2010.

15. Esram T, Chapman PL. Comparison of photovoltaic array maximum power point tracking techniques. Energy Conversion, IEEE Transactions on. 2007;22(2):439-49.

16. Myrzik JMA, Calais M. In: String and module integrated inverters for single-phase grid connected photovoltaic systems - a review. Power tech conference proceedings, 2003 IEEE bologna; ; 2003. p. 8 pp. Vol.2.

17. Kjaer SB, Pedersen JK, Blaabjerg F. A review of single-phase grid-connected inverters for photovoltaic modules. Industry Applications, IEEE Transactions on. 2005;41(5):1292-306.

18. Sherif, Raed A. Boutros, Karim S., inventor; Solar module array with reconfigurable tile. patent 6,350,944. 2002 Feb. 26.

19. Dzung Nguyen, Lehman B. An adaptive solar photovoltaic array using model-based reconfiguration algorithm. Industrial Electronics, IEEE Transactions on. 2008;55(7):2644-54.

20. Chew KWR, Siek L. In: Single inductor quad-input-dual-output buck converter for photovoltaic systems. IECON 2010 - 36th annual conference on IEEE industrial electronics society; ; 2010. p. 704-9.

21. Chang C, inventor; Solar cell array having lattice or matrix structure and method of arranging solar cells and panels. patent 6635817. 2003 Oct. 21.

22. Velasco-Quesada G, Guinjoan-Gispert F, Pique-Lopez R, Roman-Lumbreras M, Conesa-Roca A. Electrical PV array reconfiguration strategy for energy extraction improvement in grid-connected PV systems. Industrial Electronics, IEEE Transactions on. 2009;56(11):4319-31.

23. Auttawaitkul Y, Pungsiri B, Chammongthai K, Okuda M. In: A method of appropriate electrical array reconfiguration management for photovoltaic powered car. Circuits and systems, 1998. IEEE APCCAS 1998. the 1998 IEEE asia-pacific conference on; ; 1998. p. 201-4.

24. Salameh ZM, Liang C. In: Optimum switching points for array reconfiguration controller. Photovoltaic specialists conference, 1990., conference record of the twenty first IEEE; ; 1990. p. 971,976 vol.2.

25. Chaaban MA, Alahmad M, Neal J, Shi J, Berryman C, Cho Y, et al. In: Adaptive photovoltaic system. IECON 2010 - 36th annual conference on IEEE industrial electronics society; ; 2010. p. 3192-7.

26. California Energy Commission. Performance test protocol for evaluating inverters used in grid-connected photovoltaic systems. 2004.

27. Nh. Reich1, W.G.J.H.M. Van Sark, E.A. Alsema, S.Y. Kan2, S. Silvester, A.S.H. Van Der Heide, R.W. Lof, R.E.I. Schropp. In: Weak light performance and spectral response of different solar cell types. Twentieth european photovoltaic solar energy conference; Barcelona, Spain. ; 2003.

28. F. P. Baumgartner, H. Schmidt, B. Burger, R. Bründlinger, H. Häberlin, M. Zehner. In: **Status and relevance of the DC voltage dependency of the inverter efficiency**. 3-7 September 2007; Fiera Milano. "22nd European Photovoltaic Solar Energy Conference And Exhibition; 2007.

29. H. Haeberlin, L. Borgna, M. Kaempfer And U. Zwahlen. In: Total efficiency H_{tot}- A new quantity for better charachterisation of grog-connected pv inverters. June 2005; Barcelona, Spain. 20th European Photovoltaic Solar Energy Conference, Barcelona, Spain, June 2005.

30. Www.nrel.gov [Internet].: National Renewable Energy Laboratory (NREL); 2010.

31. National Fire Protection Association. National electrical code (NEC). ; 2008.

32. Effect of rooftop exposure on ambient temperatures inside conduitshttp://www.iaei.org/magazine/2009/03/effect-of-rooftop-exposure-on-ambient-temperatures-inside-conduits/ [Internet].: IAEI magazine [updated March 2009.